UNIVERSITY OF GENOA
POLYTECHNIC SCHOOL

DIME - Department of Mechanical, Energy, Management and Transportation Engineering

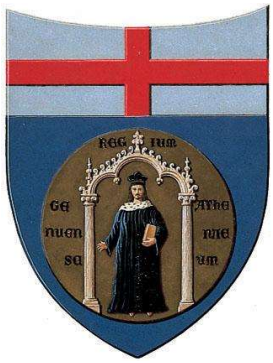

PhD in Marine Science and Technology
Technologies and System Engineering for Marine Applications

PhD Thesis
XXXV Course

"Components and Architecture optimisation for marine fuel cell systems"

Supervisor:
Prof. Aristide Fausto Massardo

Candidate:
Michele Bozzolo

June 2024

UNIVERSITÀ DEGLI STUDI DI GENOVA
SCUOLA POLITECNICA

DIME - Dipartimento di Ingegneria Meccanica, Energetica, Gestionale e dei Trasporti

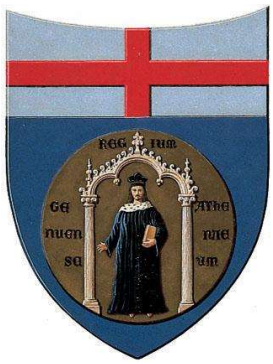

Dottorato Scienze e Tecnologie del mare
Curriculum Macchine e Sistemi Energetici per il Mare

Tesi di Dottorato
XXXV Ciclo

"Ottimizzazione di componenti e architetture di sistema per celle a combustibile in ambiente marino"

Supervisore:
Chiar.mo Prof. Aristide Fausto Massardo

Candidato:
Michele Bozzolo

Giugno 2024

Contents

List of Figures I
List of Tables II
Abstract III
Sommario IV
Acknowledgements V
Nomenclature VI
1 Introduction 1
1.1 Background 1
1.2 Regulations 4
1.3 The case for hydrogen propulsion 8
2 Electrification of marine propulsion systems based on fuel cell modules 10
2.1 Fuel Cell Technologies 10
2.1.1 Polymer Electrolyte Fuel Cells 10
2.1.2 Solid Oxide Fuel Cells 12
2.2 Electrification of marine propulsion 13
2.3 Fuel cell modules: state of the art and compatibility with marine application 16
3 The Design of a fuel cell module 20
3.1 Fundamental design parameters and their interactions 20
3.2 Pressurisation 23
3.3 Functional definition of subsystems and components 25
3.3.1 Air subsystem 25
3.3.2 Fuel subsystem 26
3.3.3 Cooling subsystem 28
3.3.4 Electrical subsystem 29
3.3.5 Control subsystem 30
3.3.6 Mechanical subsystem 31
4 Definition of a fuel cell module design 32
4.1 Sizing of the main components 32
4.1.1 Fuel cell stack 32
4.1.2 Air subsystem 35
4.1.3 Fuel subsystem 38
4.1.4 Cooling Subsystem 39
4.1.5 Electrical Subsystem 39
4.2 The modelling environment 41
4.2.1 Main modelling assumptions 42
4.2.2 The case study 44
4.2.3 Model overview 45
5 Analysis of the module operation 48
5.1 Performance of the fuel cell stack 48
5.2 Fuel Subsystem Behaviour 50
5.3 Air Subsystem Behaviour 54
5.4 Cooling Subsystem Behaviour 59

5.5 Module Performance 61
6 Conclusions 62
6.1 Opportunities for further improvement 64
Bibliography 65

List of Figures

Figure 1: World transport sector energy demand [2]. 2
Figure 2: world maritime energy demand previsions by carrier [2]. 2
Figure 3: use of alternative fuels for the world fleet by June 2021: ships in operation and on order are considered [3]. 4
Figure 4: world mapping of ECAs at 2020 [4] 5
Figure 5: Global transport sector energy consumption by fuel [5]. 7
Figure 6: CO_2 emission reductions by mitigation category and TRL [5] 8
Figure 7: Basic architecture of an electrified propulsion system comprising three fuel cell modules 15
Figure 8: Fuel cell module subsystems 16
Figure 9: the cellcentric BZA150 moduled designed for truck application 18
Figure 11: Interaction between fuel cell module design parameters 21
Figure 12: Example of a generic cell performance curve 23
Figure 13: Reference cell performance assumed in the analysis 33
Figure 14: The Fischer EMTCT-120K 35
Figure 15: Reference compressor map published by Fischer 36
Figure 16: Example of a hollow fiber air humidifier: Fumatech 100N 37
Figure 17: Main components within the air system and their relative location 38
Figure 18: Lookup tables regulating E-TC speed, By-pass valve opening and coolant pump speed 43
Figure 19: Operational schedule of the purge valve 44
Figure 20: Stack load profile 45
Figure 21: Model overview in GT-Suite 46
Figure 22: Stack voltage 48
Figure 23: Stack LHV Efficiency 49
Figure 24: Purge flow and effect on pressure 50
Figure 25: Effect of purge cycles on anode outlet gas composition 52
Figure 26: Anode stoichoimetry 53
Figure 27: Trace on the compressor map (see fig.15) 54
Figure 28: Depressurisation of the air subsystem 55
Figure 29: E-TC Performance 56
Figure 30: Cathode stoichiometry (lambda) 57
Figure 31: Relative humidity control and humidifier by-pass valve 58
Figure 32: Stack coolant temperatures 59
Figure 33: Coolant pump flow and trace 60
Figure 34: Stack and module performance 61

List of Tables

TABLE 1: NO_x EMISSION LIMITS AT TIER REGULATION 6
TABLE 2: MOST RELEVANT FUEL CELL TECHNOLOGIES 10
TABLE 3: HYDROGEN PURITY FOR PEM FUEL CELL USE [6] 11
TABLE 4:FUEL CELL MODULE SUBSYSTEMS AND THEIR FUNCTIONS 17
TABLE 5: LIST OF PARAMETERS DEFINING A STACK PERFORMANCE CURVE 24
TABLE 6: AIR SUBSYSTEM COMPONENTS AND FUNCTIONS 26
TABLE 7: FUEL SUBSYSTEM COMPONENTS AND FUNCTIONS 27
TABLE 8: COOLING SUBSYSTEM COMPONENTS AND FUNCTIONS 29
TABLE 9: ELECTRICAL SYSTEM COMPONENTS AND FUNCTIONS 30
TABLE 10: CONTROL SUBSYSTEM COMPONENTS AND FUNCTIONS 31
TABLE 11: MECHANICAL SUBSYSTEM COMPONENTS AND FUNCTIONS 31
TABLE 12: REFERENCE POINT FOR THE SIZING OF THE ANODE EJECTOR 39

Abstract

The energy transition to zero emission maritime transport implies a central role for hydrogen as an energy carrier of choice for multiple applications and use cases. Among the power conversion technologies fuel cell systems can combine unrivalled performance and zero tailpipe emission.

Nonetheless the state-of-the-art architectures of fuel cell modules are largely driven by requirements related to the on-road applications, while the maritime applications with their specific performance indicators are expected to be suitable for alternative designs.

In this context, the thesis is focusing on the architecture of the fuel cell module, the fundamental functions carried out by the subsystems within it and the design choices to be made in a defining an architecture suitable for installation in conjunction with a marine propulsion system.

Moreover, the defined design is modelled and analysed to evaluate its performance and the ability of all subsystems to perform the assigned functions, at steady state and in transient conditions.

Sommario

La transizione energetica verso un trasporto marittimo a zero emissioni determina un ruolo centrale per l'idrogeno come vettore energetico per molteplici applicazioni ed esempi d'uso. Tra le tecnologie di generazione elettrica, i sistemi a celle a combustibile possono offrire eccellenti prestazioni in combinazione con zero emissioni dallo scarico.

Tuttavia, le architetture dei moduli di celle a combustibile che oggi rappresentano lo stato dell'arte sono in gran parte determinate da requisiti relativi alle applicazioni su strada, mentre le applicazioni marittime con i loro specifici indicatori di prestazione possono essere meglio soddisfatte da configurazioni alternative.

In questo contesto la tesi si concentra sull'architettura del modulo di celle a combustibile, sulle funzioni fondamentali svolte dai sottosistemi al suo interno e sulle scelte progettuali da operare nella definizione di un'architettura adatta all'installazione in accoppiamento con un sistema di propulsione marina.

Inoltre, il progetto definito viene modellato e analizzato per valutarne le prestazioni e la capacità di tutti i sottosistemi di svolgere le funzioni assegnate, in condizioni stazionarie e transitorie.

Acknowledgements

I would like to express my deepest appreciation to Professor Massardo for his coaching and example over the course of more than twenty years so far. My professional career has been and still is positively influenced by his effort and support.

I would like to extend my sincere thanks to Professor Arnulfi and Professor Gambarotta for the patience and effort spent in reviewing my work.

Listing all the coaches, colleagues and friends who supported me since my graduation in 2001 at Rolls-Royce, LG, at the University of Genoa, and in all partner companies throughout my professional career so far would be next to impossible and too high would be the risk of neglecting someone. I simply hope I have given them enough in exchange for what I've been learning from them.

And to Kaja, Piwo and Puszek.

Nomenclature

Abbreviations and Acronyms

BES	Battery Energy Storage
BoP	Balance of Plant
CC	Capital Cost
COP	Coefficient Of Performance
CP	Centrifugal Pump
DSB	Dry-Side Bypass valve
EEA	European Environmental Agency
EG	Electrical Generator
EM	Electrical Motor
EMSA	European Maritime Safety Agency
ET	Expansion Tank
E-TC	Electrically driven Turbocharger
FCB	Fuel Cell Bypass valve
GHG	Green House Gases
GTG	Gas To Gas heat exchanger
HX	Heat Exchanger
HPR	Hydrogen Pressure Regulator
HRB	Hydrogen Recycle Blower
HUM	Humidifier

IMO	International Maritime Organization
LMTD	Logarithmic Mean Temperature Difference
LNG	Liquid Natural Gas
MEPC	Marine Environment Protection Committee
PEMFC	Polymer Electrolyte Membrane Fuel Cell
PID	Proportional Integral Derivative
SCB	Side Channel Blower
TC	Turbo Charger
TRL	Technology Readiness Level
TV	Thermostat Valve
WSHE	Water-Sea Heat Exchanger

Variables

A	Area [m^2]
C_f	Pressure drops friction coefficient [-]
c_p	Specific heat for constant pressure [J/kg K]
D	Diameter [m]
$E_{cell,ideal}$	Nernst theoretical voltage [V]
F	Faraday constant [C/mol]
G	Specific density [-]
H	Head [m]
h	Enthalpy [J/kg]
I	Current [A]

J_{N_2}	Nitrogen diffusion rate [mol/s /bar]
K	Conductive heat transfer coefficient [W/m/K]
k	Heat capacity ratio [-]
L	Length [m]
M	Mass [kg]
$\dot{m}$	Mass flow [g/s]
MM	Molar mass [g/mol]
N	Rotational speed [rpm]
n_{cell}	Number of cells [-]
OF	Opening Fraction[-]
P	Power [W]
p	Pressure [Pa]
Q	Heat flux [W_{th}]
$\dot{Q}$	Volumetric flow [m^3/s]
R	Universal gas constant [J/mol/K]
Re	Reynolds number [-]
RH	Relative humidity [-]
T	Temperature [°C,K]
t	Time [s]
U	Global heat exchange coefficient [$W/m^2/K$]
v	Volume [m^3]
WTR	Water Transfer Rate across humidifier [g/s]
x	Volumetric gas fraction [-]

Greeks

α	Charge transfer coefficient [-]
β	Pressure ratio [-]
γ_{act}	Activation voltage loss [V]
γ_{conc}	Concentration voltage loss [V]
γ_{ohm}	Ohmic voltage loss [V]
σ_m	Cell membrane resistance [A m^2/V]
η	Efficiency [-]
λ_{mem}	Membrane water content [-]
ρ	Density [kg/m^3]

Subscripts and Superscripts

AN	Anode
CA	Cathode
$COLD$	Relative to cold fluid
$cool$	Cooling
dew	Dew Point
$diff$	Diffusion
el	Electrical
HOT	Relative to hot fluid
is	Isentropic
ref	Reference conditions
st	Relative to the stack

1 Introduction

1.1 Background

The European economy relies significantly on the maritime transport sector, which handles 77% of total overseas and 35% of internal European trade. Despite a downturn in maritime activity in 2020 due to the COVID-19 pandemic, future growth is anticipated, driven by increasing demand for primary resources. A recent report by the European Environment Agency (EEA) and the European Maritime Safety Agency (EMSA) offers a comprehensive analysis of the environmental impact of European maritime transport, revealing that ships contribute 13.5% of the EU's greenhouse gas emissions, ranking third after road transport (71%) and aviation (14.4%). [1]

In 2019, ships docking in European harbors emitted approximately 1.63 million tons of sulfur dioxide (SO2). These emissions, stemming largely from fossil fuel combustion, contribute significantly to air pollution and climate change, as the marine transport sector remains one of the least regulated anthropogenic emission sources. Moreover, ships calling at ports in the EU and the European Economic Area emitted an estimated 140 million tons of CO2 in 2018, constituting around 18% of total worldwide emissions.

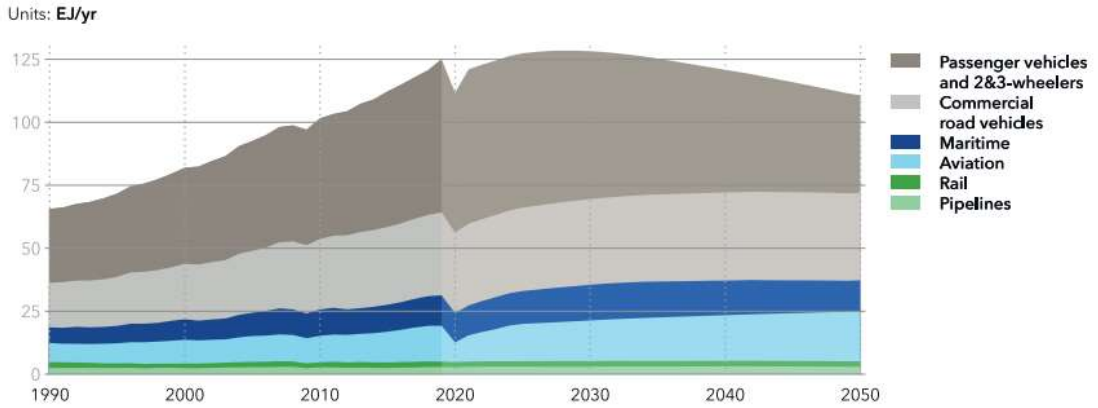

Figure 1: World transport sector energy demand [2].

Ships currently consume almost 3% of the world's final energy demand and 7% of world oil, particularly for international goods transport. By 2050, there will be a shift in fuel composition, with zero-carbon or alternative fuels like ammonia, hydrogen, and methanol comprising 42%, and natural gas, particularly LNG, making up 39%. The International Maritime Organization (IMO) aims to reduce greenhouse gas emissions by 50% from 2008 levels by 2050, guiding this transition. Forecasts by DNV suggest that improved energy efficiency and a significant shift to decarbonized fuels will be pivotal in achieving this objective.

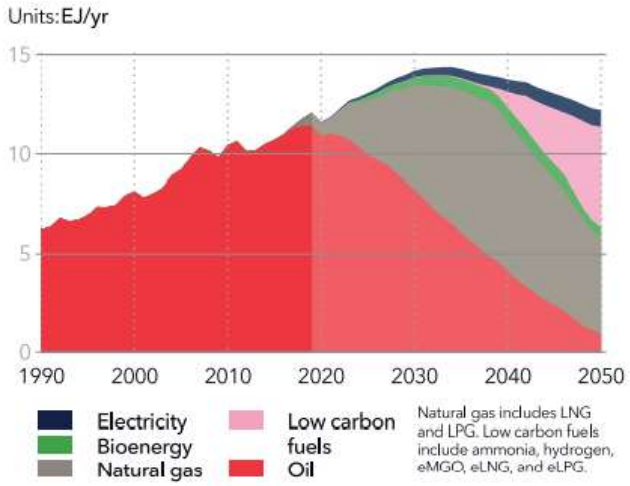

Figure 2: world maritime energy demand previsions by carrier [2].

The European Union's maritime transport sector is entering a pivotal decade marked by a transition toward enhanced economic, social, and environmental sustainability. As per the EEA report, a majority of vessels docking at EU ports have already slashed their speed by an average of 20% compared to 2008, leading to reduced emissions. Moreover, exploring alternative energy sources and fuels such as biofuels, batteries, hydrogen, or ammonia holds promise for decarbonizing the sector and achieving emission reductions down to zero. However, it is imperative from a lifecycle standpoint to ensure that the adoption of alternative fuels does not introduce further unsustainable consequences.

Presently, the IMO's regulations solely address CO2 emissions from fossil fuels from the tank to the propellor, overlooking significant emissions of methane (CH4) and nitrous oxide (N2O) from shipping. Efforts are underway to develop guidelines for determining lifecycle CO2 and GHG emission factors for all fuels, including biofuels and synthetic electrofuels, by the IMO.

According to recent findings, methanol, hydrogen, and ammonia are emerging as notable alternative fuels, particularly in the short-sea segment and non-cargo vessels. However, their current usage has minimal impact on overall maritime emissions. Nonetheless, approximately 12% of new ship constructions are opting for alternative fuel systems.

In the forthcoming years, a discernible uptick is expected in the orders for deep-sea LNG-fueled vessels globally and batteries for either full-electric or partial-electric short-sea operations. Despite the progress, most alternative fuels

remain reliant on fossil fuels, except for the ongoing electrification in the short-sea sector.

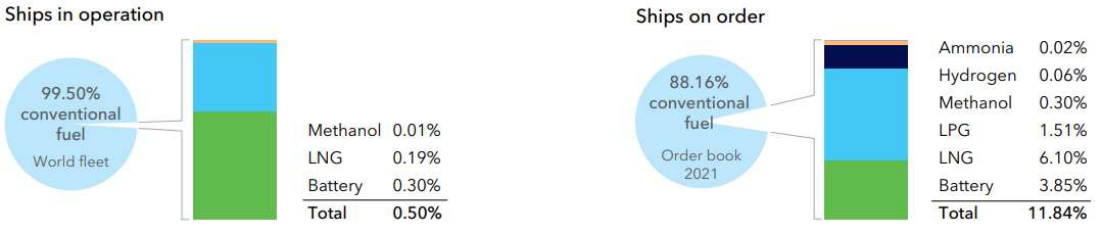

Figure 3: use of alternative fuels for the world fleet by June 2021: ships in operation and on order are considered [3].

Looking at new ship orders over the next few years, it can be underlined an increase in the number of deep-sea LNG-fueled ships worldwide and batteries for full-electric or part-electric short-sea operations. Most alternative fuels are still based on fossil fuels, with the exception of the electrification that is taking place in the short-sea segment.

1.2 Regulations

Globally, ship emissions are regulated by the International Maritime Organization (IMO), a specialized agency of the United Nations tasked with ensuring shipping safety, security, and preventing marine pollution. The IMO oversees approximately sixty legal instruments aimed at guiding the regulatory efforts of its member states to promote maritime safety, facilitate trade, and protect the marine environment, with the International Convention for the Safety of Life at Sea (SOLAS) being the most prominent among them.

Acknowledging the necessity for a regulatory framework for gas-fueled ships, the IMO initiated the development of the International Code of Safety for Gas-fueled Ships (IGF Code), which remains in progress. Regulations addressing air pollution prevention are outlined in Annex VI of the International Convention for the Prevention of Pollution from Ships (1973), later amended by the Protocol

MARPOL 73/78. These regulations became mandatory in May 2005. MARPOL Annex VI imposes limits on sulphur oxides and nitrogen oxides emitted by ships and prohibits intentional emissions of ozone-depleting substances.

Sulphur oxides (SOx) are restricted by a global cap of 4.5% on the sulphur content of fuel oil, with the IMO tasked with monitoring the average sulphur content of marine fuel worldwide. The annex includes provisions for establishing Special SOx Emission Control Areas (SECAs), where the sulphur content of fuel oil used onboard ships must not exceed 1.5%. Amendments to Annex VI, overseen by the Marine Environment Protection Committee (MEPC), have led to the establishment of Emission Control Areas (ECAs) with even lower emission limits (see Figure 4).

Figure 4: world mapping of ECAs at 2020 [4].

Specific technologies to limit the emission of sulphur oxides are required to operate in such areas, namely the Baltic Sea Area and the North Sea, designated as Sox Emission Control Areas.

Table 1: NO_x emission limits at Tier regulation

Tier	Ship build date	Limit on total weighted cycle emissions		
		Engines speed <130rpm	130rpm< Engines speed <1999rpm	Engines speed >1999rpm
I	1st January 2000	17	$45\,n^{-0.2}$	9.8
II	1st January 2011	14.4	$44\,n^{-0.23}$	7.7
III	1st January 2016	3.4	$9\,n^{-0.2}$	2

The regulation concerning oxides of nitrogen (NOx) is addressed in Annex VI through a mandatory technical code, which outlines procedures for testing, surveying, and certifying marine diesel engines. In 2008, the IMO set a target of reducing NOx emissions by 30% compared to 1990 levels. The existing regulation, known as Tier I, imposes emissions limits of 17 g/kW h for engines operating at the lowest rated speeds above 2000 rpm. Tier II (ranging from 14.4 to 7.7 g/kW h) applies to engines built on or after January 1, 2011, while Tier III (ranging from 3.4 to 2.0 g/kW h) applies to engines constructed after January 1, 2016 (see Table 1). When operating within a designated emission control area, Tier III regulations must be adhered to; otherwise, Tier II limits apply.

The MEPC has recognized the need for action on greenhouse gases (GHG) and has proposed various short- and long-term measures. However, until 2018, no mandatory restrictions had been placed on CO2 emissions. In April 2018, the IMO adopted an ambitious strategy to reduce greenhouse gas (GHG) emissions from shipping. The preliminary goal is to decrease carbon dioxide (CO2) emissions by at least 40% per cargo tonne-mile by 2030 (with a target of 70% reduction by 2050) and to achieve a 50% reduction in overall GHG emissions by 2050, compared to 2008 levels. The 2030 reduction targets are demanding but,

as they measure carbon intensity, they allow for trade growth. However, any measures taken to meet these objectives must also account for the 2050 targets to accommodate the growth in trade and transportation demand while reducing GHG emissions. This necessitates the development of new technologies.

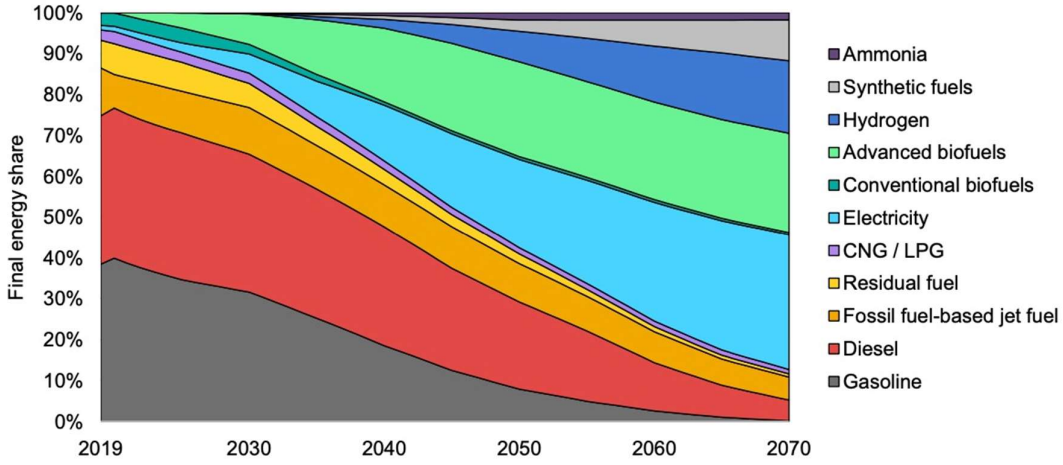

Figure 5: Global transport sector energy consumption by fuel Error! Reference source not found..

The IEA, International Energy Agency, estimates [5] the cost of the transition to zero emission shipping could reach 6 trillion US dollars in the next 50 years.

Moreover, according to the IEA the stated policies can only limit the growth of the global emissions and a transition to the wide use of Hydrogen and Ammonia is required together with performance optimization to achieve a long term reduction in a continuous growth scenario.

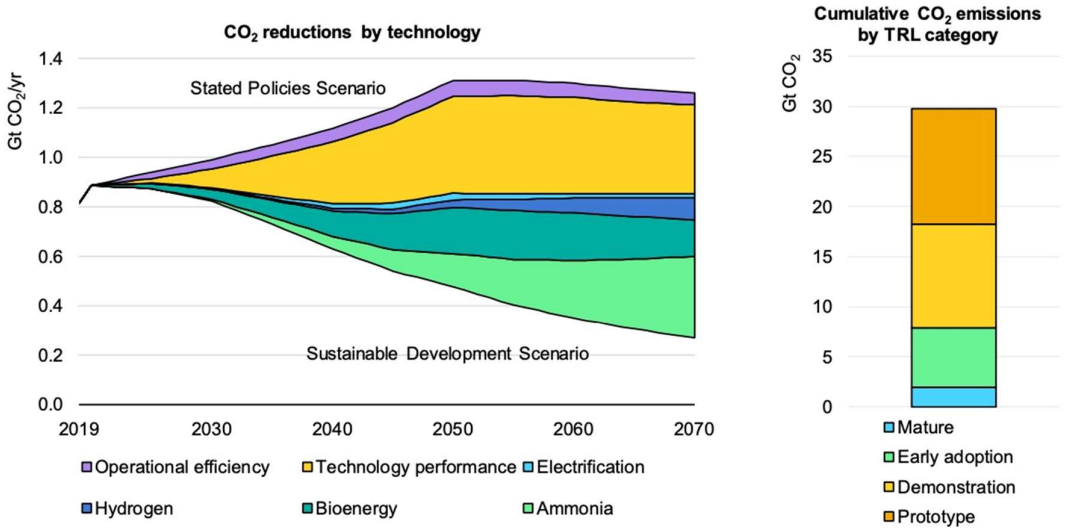

Figure 6: CO_2 emission reductions by mitigation category and TRL Error! Reference source not found..

1.3 The case for hydrogen propulsion

A prerequisite for the introduction of a radically new fuel in marine propulsion, with the huge associated investment in hardware and infrastructure is a disruption of the present state-of-the-art portfolio of solutions. Emission regulations are certainly a key constraint, but the mechanism by which such constraint reflects into the market is an increase of total cost of ownership for the vessel operator.

In general, not all use cases and applications can be easily targeted for hydrogen-based propulsion systems. Compared to other liquid synthetic fuels its volumetric power density is inferior, making it a less favourable option for long range/large scale applications. Nonetheless, most processes to synthesize such fuels are based on hydrogen as a fundamental building block, therefore any additional process will result in a cost penalty over the direct use of hydrogen as a fuel.

Given the size of the investments required for the transition to happen, and the poorer characteristics of hydrogen compared to traditional fuels in terms of

energy storage, power conversion efficiency is expected to become a key parameter influencing the total cost of ownership of the vessel.

In such scenario a substantial opportunity will open for fuel cells, starting from the short-sea segment and above, in use cases where a battery electric solution cannot meet the requirements in terms of range, operating schedules or, again, total cost of ownership.

2 Electrification of marine propulsion systems based on fuel cell modules

This section provides a brief overview of the most promising architectures of electrified propulsion systems for marine application. The focus will be on technologies that are most suitable for integration with Hydrogen-fueled power generation systems, and fuel cell modules in particular. In all the configurations considered a propellor is assumed to be the vessels' mean of propulsion.

2.1 Fuel Cell Technologies

Many different fuel cell technologies have been developed over the years, often, while similar in functionality, wildly different in terms of material sets, mechanical design, operating conditions and suitable reactants.

Table 2: Most relevant fuel cell technologies

	AFC	PAFC	MCFC	SOFC	PEMFC
Electrolyte	Potassium hydroxide	Phosphoric Acid	Molten carbonate salt	Ceramic	Polymer
Operating Temperature	60-200 °C	140-200 °C	650-800 °C	500-1000 °C	60-180 °C
Fuel	H_2	H_2/LNG/CH_4 reformate	H_2 /CH_4 reformate	H_2 /CH_4 reformate	H_2

Out of the most relevant technologies two in particular are considered as the most promising for marine application:

2.1.1 Polymer Electrolyte Fuel Cells

PEM fuel cell technology is the most mature of all fuel cell technology, having most manufacturers globally converged to consistent a state-of-the-art design. While some manufacturers concentrate their efforts towards higher

temperature capable membrane materials (HT-PEM) most stacks rely on the evolution of a fluorinated Teflon-based material originally developed by DuPont for NASA in the 960s.

The choice of bi-polar plate material is possibly the main differentiator between manufacturers as of today, some preferring the higher durability of carbon-composite plates others pursuing the higher mechanical robustness and lower thicknesses of metal based solutions, often relying on coatings to achieve the desired durability.

Liquid cooling is the most common choice for stack temperature control with only a handful of manufacturers offering air-cooled small stacks or evaporatively cooled cathode channels.

LT-PEM fuel cell stacks are today the most power dense, reaching 5-6 kW/l and durability in excess of 50000 hours.

The main constraint posed by such technology is the compatibility with only high purity Hydrogen as a fuel with an extremely low tolerance to specific contaminants, carbon monoxide in particular.

Table 3: Hydrogen purity for PEM fuel cell use [6]

Contaminants	ISO 14687 (D) (ppm)
Water	5
Total hydrocarbons except methane	2
Methane	100
Oxygen	5
Helium	300
Nitrogen	300
Argon	300
Carbon dioxide	2
Carbon monoxide	0.2
Total sulphur compounds	0.004
Formaldehyde	0.2
Formic Acid	0.2
Ammonia	0.1
Halogenated compounds	0.05

Such fundamental constraints constitutes a practical limit for the application of such technology in the marine to hydrogen-fuelled vessels. Although

technologies are being developed allowing the onboard production of high purity hydrogen from liquid fuels of synthetic or fossil origin, the additional cost and complication makes the combination of these two systems unattractive compared to internal combustion engines directly fed with such liquid fuels.

Nonetheless, hydrogen fed LT-PEM fuel cell systems will be the solution considered in this work.

2.1.2 Solid Oxide Fuel Cells

SOFCs stacks operating at temperatures higher than 600°C upto 900°C and beyond can be fueled by a wide range of combustible mixtures, including hydrocarbons and ammonia as well as hydrogen.

Fuel compatibility and excellent conversion efficiency are the key performance indicators promoting the development of this technology, however the manufacturers have not yet converged to a single state-of-the-art design.

The commercially available stacks today fundamentally vary in material set, mechanical design, operating temperature, operating pressure and dynamic response capabilities.

In general, today's SOFC offer inferior power density compared to LT-PEMs, lower durability and higher costs.

While the requirement for high temperature operation offers opportunities for thermal integration and recuperation with/from other systems it makes the mechanical design fundamentally more complex and less power dense.

Finally, slower dynamics are inherent with the complex thermal management of such systems, making them less attractive for integration into marine propulsion systems as a standalone technology.

Nonetheless, hybrid solutions in combination with ICEs or other power conversion technologies [7], where the SOFC can be optimised to provide excellent baseload efficiency, can be extremely advantageous.

2.2 Electrification of marine propulsion

A small to medium-sized marine vessel is in general designed including a number of independent and redundant propulsion systems to ensure operability in the widest range of conditions. The most common propulsion system designs rely on a direct or indirect mechanical connection between a propellor and a prime mover, commonly and internal combustion engine.

In an electrified marine propulsion system the propellor is powered exclusively by an electric motor. Such motor is in general assumed to be connected to a DC power source via a variable-speed-capable motor controller unit, but depending on the vessel, its mission and the relative requirements, multiple configurations of subsystems could perform the function of such power source. In particular three families of architectures are of interest

- Electrical Energy Storage System: Generally a battery to be recharged in harbours. Such solution is considered to be extremely attractive for specific vessels and use cases due to its zero tailpipe emissions, as well as extremely high power conversion efficiencies, as no power generation takes place on the vessel. On the other hand, such solution is fundamentally limiting the range of mission for the vessel and its capabilities. Large battery sizes will be required for long range missions with the associated cost and weight/volume constraints. A thorough analysis of the vessel duty cycles, an accurate customisation effort, and more importantly, an acceptance of operational limitations on the vessel operator's side are a prerequisite for the viability of such solution. This latter aspect in particular can have crucial impact on the end customer as it may result in a redefinition of the operational strategy for an entire fleet of vessels, impacting logistics, personnel and the viability of the overall business case. Typical ideal cases for such solution are ferries

rigidly operated on fixed schedules and routes, particularly in small bodies of water.

- Internal combustion engines (ICE) or gas turbines (GT) [8] [9]: In such configurations power is generated onboard the vessel and transformed to feed a DC bus connected to the motor control unit driving the propellor's motor. As the most commonly employed power generation technologies include an electrical generator spinning at a given shaft speed a rectifier will be required to convert the produced AC power into DC. An energy storage device, albeit of limited capacity, will be almost always considered as part of the architecture to improve the dynamic response of the overall system, being ready to deliver power while waiting for the power generation units' response. Such architectures are fundamentally compatible with a wide range of fuels, of fossil, biological or synthetic origin, and each specific configuration will determine the associated tailpipe emissions. From the customer's perspective such architectures can be attractive as they do not necessarily constrain the operational schedule of the vessel. On the other hand, the advantages over a mechanical or hybrid propulsion systems can be rather limited with the increased cost associated to the power conversion from mechanical into electrical and again into mechanical power. Moreover, configurations operated with carbon-containing fuels will produce a CO2 emission at the tailpipe, and even when operated with ammonia [10] or pure hydrogen, undesirable pollutants, namely NOx, will be produced as part of the combustion process in non-neglectable amounts.
- Fuel cell modules (FCM) [11] [12]: in such configurations the source of DC power is a single or multiple fuel cell modules. A fuel cell module is a system including one or multiple fuel cell stacks and all the subsystems required for its operation. Each fuel cell stack can perform the electrochemical oxidation of the fuel directly producing DC power. Moreover, fuel cells offer extremely high conversion efficiencies, up to and

in some cases above 60% and, if fuelled with pure hydrogen, the tailpipe emissions are just water, in vapour or liquid form. Many types of fuel cell technologies have been developed, each associated with different operational temperatures, power densities, performance, maturity, and, in general, all key performance indicators that determine their suitability to each given application. This work focuses on the low temperature polymer electrolyte fuel cell technology, as an attractive solution for marine applications, due to its high degree of maturity, excellent dynamic response and very good power density. Consequently, as such technology, with limited exceptions, can only operate on pure hydrogen, such fuel only will be considered for the remainder of this work.

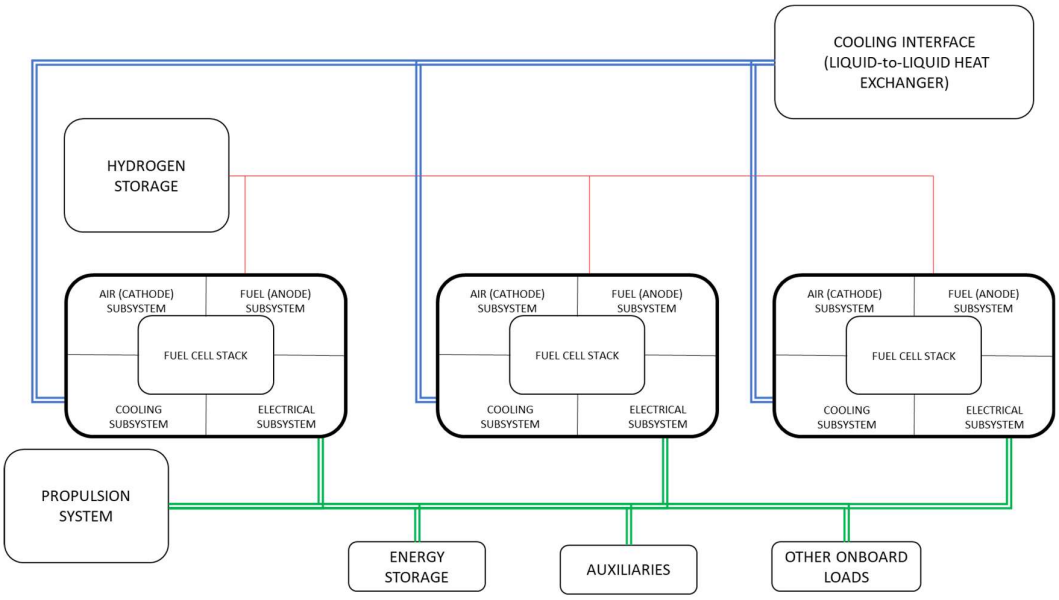

Figure 7: Basic architecture of an electrified propulsion system comprising three fuel cell modules

2.3 Fuel cell modules: state of the art and compatibility with marine application

A fuel cell module is a system comprising at least a fuel cell stack and all the subsystems required for its operation. From a functional perspective, the four main subsystems are those required to manage the four interfaces of the fuel cell stack: anode side, cathode side, coolant and electrical.

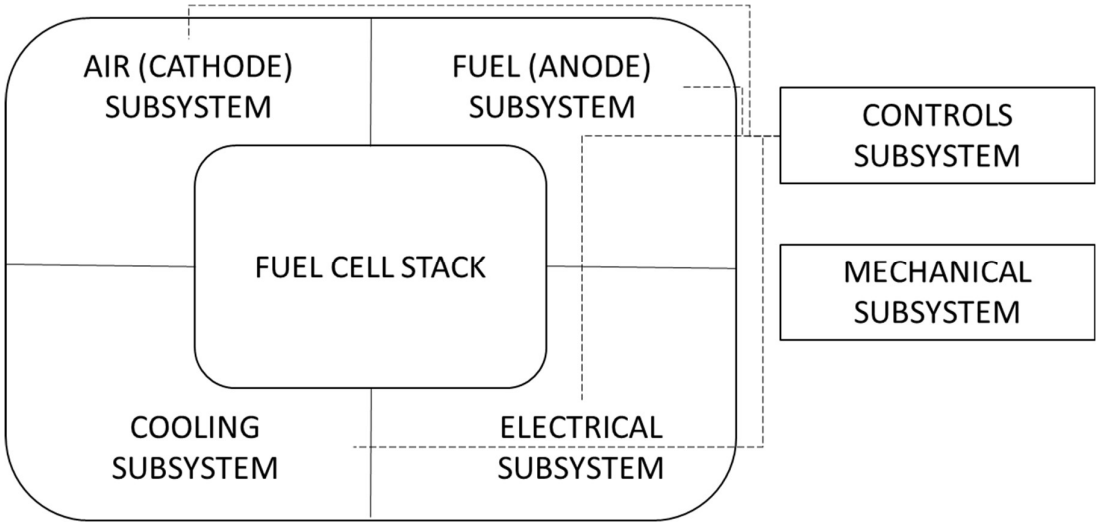

Figure 8: Fuel cell module subsystems

In addition, a control system is required to ensure the module operates safely while satisfying the performance requirements

Finally, a mechanical subsystem can be defined as constituted of all components designed to maintain integrity in operation.

Table 4:Fuel cell module subsystems and their functions

Subsystem	Function
Fuel cell stack	To generate DC power converting Hydrogen and Oxygen into water
Air subsystem	To produce and maintain a flow of oxidising reactants to the cathode side of the fuel cell, in a suitable range of temperature, pressure and humidity
Fuel subsystem	To produce and maintain a flow of reducing reactants to the anode side of the fuel cell, in a suitable range of temperature, pressure and humidity
Cooling subsystem	To maintain the fuel cell stack and all components in the module within the correct operational temperature range
Electrical subsystem	To transfer the commanded amount of electrical power from the fuel cell stack to the external load and the internal module components
Control subsystem	To operate the module, the subsystems and the components within them according to a predefined operational strategy ensuring safety
Mechanical subsystem	To ensure the mechanical integrity of the system in operation

Specifically for the case of a low temperature polymer electrolyte fuel cell system, the on-road applications have driven the development of fuel cell modules in recent times more than any other.

In the recent years in particular, the focus has moved for many manufacturers from passenger cars to van, buses and trucks. Such shift in priority was partially driven by the widespread introduction of battery electric vehicles (BEV) in the passenger car segment and partly as a mean to address the issue of the availability of a refuelling infrastructure.

Companies managing fleets of vehicles, often operated on a 24/7 basis or on very long range missions, are seen as an attractive commercial target as they can more rapidly constitute a critical mass for the development of such infrastructure while the corresponding BEV alternative solutions are often operationally more constraining.

Such applications often determine challenging requirements in terms of gravimetric and, even more so, volumetric power density to enable installation

within a vehicle, in alternative to traditional internal combustion engines on a shared platform.

On the other hand, full power efficiency is not a key performance indicator as the fuel cell modules are generally installed in combination with a generously sized battery system and operated at relatively low and stable loads for most of their operational life.

This, together with the need of designing a cost competitive solution against the traditional ICEs has driven the choices of many module developers towards smaller pressurised stack designs, somehow driving the development of more complex subsystems and minimising the stack volumes and costs.

As a consequence, the design of fuel cell modules in recent years was driven towards mechanically integrated configurations, architectures that could be defined as “fuel cell engines”.

Figure 9: the cellcentric BZA150 moduled designed for truck application [13]

A common generic design capable of satisfying all marine applications' requirements is clearly impractical as these can be wildly different to each other.

Even with conventional systems, as an example, a tugboat requiring very infrequently vast amounts of power and a passenger ferry, mostly cruising at constant speed will drive the design of the power and propulsion systems in radically different directions.

Nonetheless, some of the radical choices made by the developers of on-road systems are not producing an added value in a marine installation and could even be considered counterproductive.

In particular, while pressurisation as a mean to maximise stack performance and specific cost can still be considered advantageous the requirements driving the trade-off between stack volume and module efficiency towards minimising volumes are hardly justified in most marine applications.

An outstandingly efficient propulsion system can be a practical way to maximise the vessel's range, or minimise the required onboard fuel storage capacity, requirements often more crucial to customers than the installation volume occupied by the fuel cell module in the engine room.

Based on the considerations above the off-the-shelf automotive/truck designs are not ideally suitable for integration with a marine propulsion system and the work will focus on the design of a fuel cell module optimised for such application.

3 The Design of a fuel cell module

A common misconception regarding fuel cell systems is the tendency to approach them as electrical systems supported by auxiliary thermodynamic subsystems, similarly to battery storage systems.
Such approach fails to address the problems arising from the nature of the fuel cell as a power conversion device, the way the subsystems interact with each other and with the stack they are serving.
The design of the fuel cell module as a single integrated system, is the key to outstanding key performance indicators in terms of power density, equipment cost and dynamic response capabilities above all.
The fuel cell system should in fact be viewed as a thermodynamic system actuated by an electrical system.

3.1 Fundamental design parameters and their interactions

The fundamental performance of a fuel cell model is influenced by a relatively small number of design parameters set in the early concept definition phase. As visible in the diagram below, showing the interdependencies of the design parameters within a fuel cell module, one key functional design parameter is the choice of the cell operating current.
Any given stack design is in general operable in a wide range of conditions, defined at the interface to the four main subsystems: air, fuel, cooling and electrical. The choice of the operating point of the stack determines the requirements for all subsystems, but the operating current has a direct impact on all of them, as all reactants' consumptions are directly proportional to it.

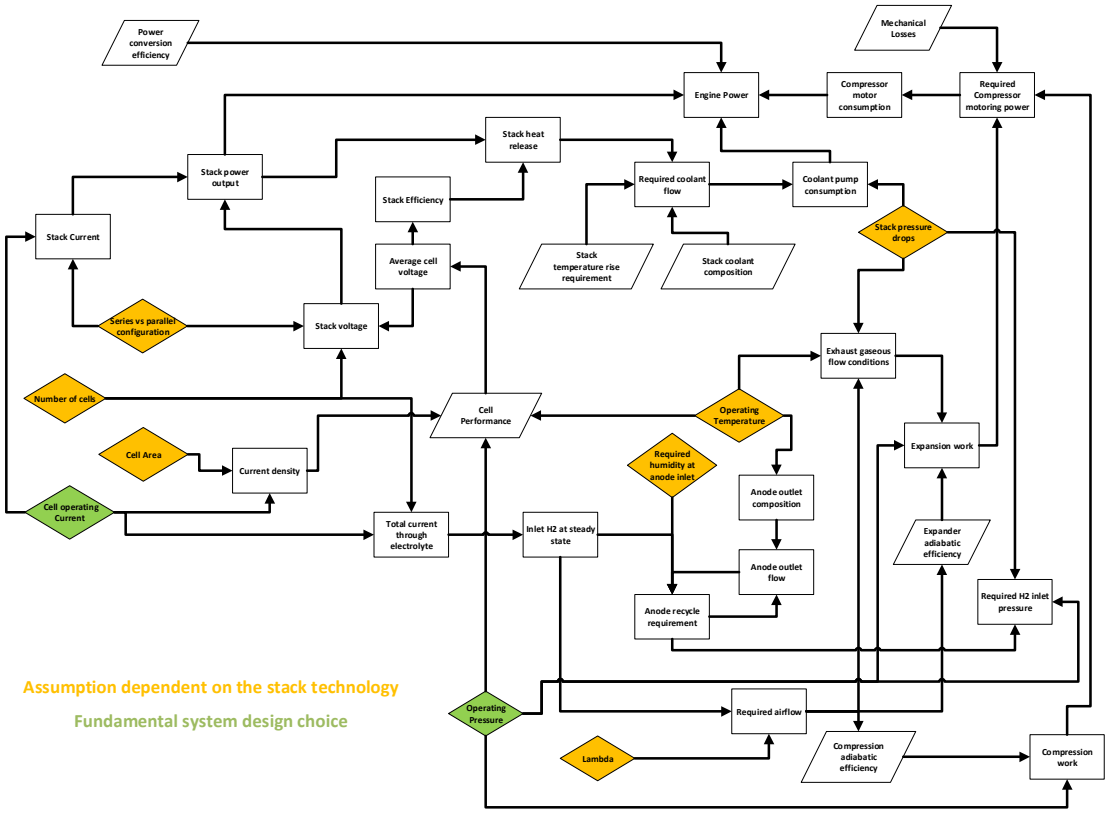

Figure 10: Interaction between fuel cell module design parameters

This is intrinsic in the nature of the fuel cell as to each electron flowing through the electrical load corresponds a proton moving through the membrane. Correspondingly, each proton will have to be provided by a hydrogen atom delivered by the fuel system and it will leave the system once combined in pairs to an oxygen atom delivered by the air system.

As a consequence, the choice of operating current not only drives the design of all subsystems in the concept definition phase, but also determines the operating point of the module in operation being it a measure of the intensity of the power conversion process. In this sense, the operating current is the actuator to the subsystems.

Voltage, on the other hand, is the true measure of cell performance, as it is proportional to conversion efficiency due to the linear relationship between fuel consumption and current.

$$\eta = \frac{IV}{LHV\ \dot{m}_{H2}}$$

Hence, given $\dot{m}_{H2} \propto I$, **(1)**

$$\eta \propto V$$

Cell voltage, and consequently module efficiency, is influenced by most of the design parameters within the stack and the subsystems.

If the choice operating current is the initial step of the concept definition, cell voltage is the last, and it can only be determined as a consequence of the definition of all other parameters.

This is noticeable in the interaction diagram, neglecting the minor effect on the sizing of the cooling system, dependent mainly on current and less so on cell voltage.

All considerations so far are somehow independent from the fundamental cell performance, defined as the relationship between cell current density and cell operating voltage. This is because such parameter influences the design of the module only in combination with the choice of the stack size, both in terms of cell active area and number of cells in the stack.

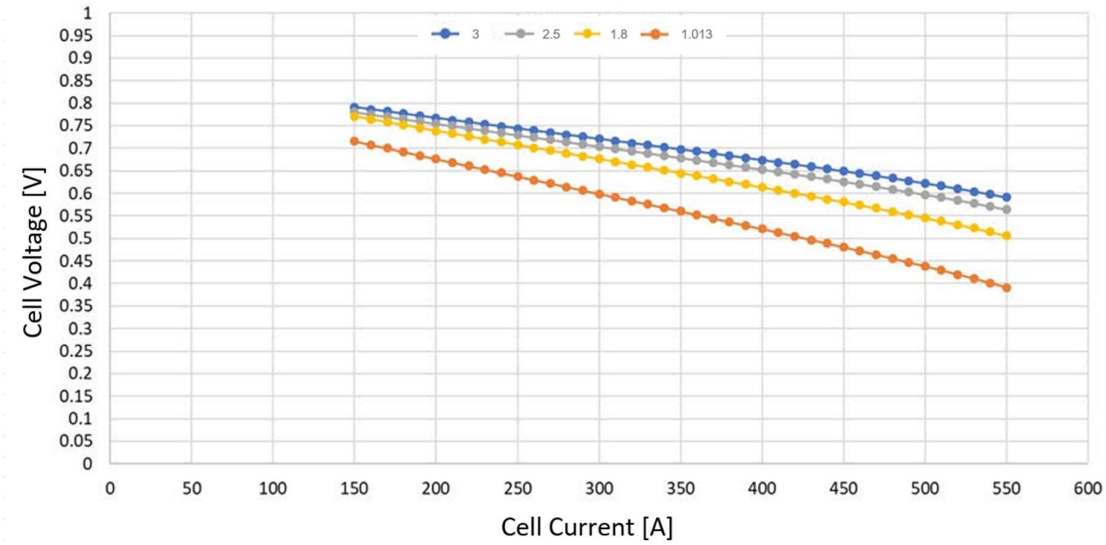

Figure 11: Example of a generic cell performance curve as a function of pressure in bar a

In practice, a smaller better performing stack could be equivalent for the functional design of the module, to a larger one made of poorer performing cells if the sizing of the latter results in an identical combination of operating current and cell voltage.

3.2 Pressurisation

The design pressure of the fuel cell module is a key parameter, and it strongly influences the choices made in defining its architecture, particularly so for the air system.

The fuel cell performance curves describe the relationship between operating current and cell voltage in a specific set of reference conditions.

Each curve is only defined at steady state and for specific defined values of the following parameters.

Air system	Fuel System	Cooling System
Air inlet Temperature	Fuel inlet pressure	Coolant inlet temperature
Air inlet relative humidity	Fuel inlet humidity	Coolant outlet temperature
Air inlet Pressure	Fuel inlet temperature	
Air stoichiometry	Fuel Stoichiometry	
	Fuel dilution	

Table 5: List of parameters defining a stack performance curve

Given the constraints above, performance curves are useful data to assess the intrinsic quality of the performance of a stack, but they cannot be directly used within a fuel cell module model as they do not provide information about the sensitivity to variations in the parameters listed above.

When multiple curves are shown, often each one describes stack performance at a different operating pressure.

Operating pressure has a strong influence on the current that can be drawn from the stack at a target voltage, corresponding to a target conversion efficiency.

As visible in the figure while operated at a typical pressure of 2.5 bar absolute a stack can produce twice the power produced in atmospheric conditions at the same efficiency.

The perspective of producing more power out of a stack of a given size and cost has driven many manufacturers to the design of pressurised fuel cell modules.

Such choices have heavily influenced not only the design of the stack itself, with a strong preference for more robust metal-based designs of bi-polar plates but has determined new challenges and opportunities in the design of the subsystems as well, the air subsystem in particular.

The air compression device is often the largest power consumer within the fuel cell module and its impact on the performance of the entire module increases at higher operating pressures. This has driven some manufacturers towards mild

pressurisation of their modules, based on a simple electrically motored compressor generally at pressure ratio lower than 2.

Alternatively, some other manufacturers have chosen instead to design turbocharged modules, recovering part of the compression work exploiting on the expansion work provided by the fuel cell off-air.

Several manufacturers are now offering specifically designed motorised turbochargers for PEM fuel cell systems, designed on oil-free bearings to avoid chemical contamination of the catalyst layers within the stack, and suitable for modules in the 60-200kWe power output range, at operating pressures up to 3 bar absolute.

Modules of smaller size are often based on the simpler compressor-only architectures, atmospheric or mildly pressurised.

3.3 Functional definition of subsystems and components

Each of the subsystems is designed to perform its function as described in table 2 by the combination of one or many components, each performing a dedicated subfunction required by the subsystem operation.

the library.

3.3.1 Air subsystem

As mentioned before, the air subsystem is designed to produce and maintain a flow of oxidising reactants to the cathode side of the fuel cell, in a suitable range of temperature, pressure and humidity.

Such high-level function can be divided into a number of component level functions required. The allocation of the functions and the choice of the components tasked to deliver them is an early concept choice defining the first step from a functional architecture towards a mechanical architecture.

In the system object of this study a turbocharged, pressurised module architecture was selected. A charge air cooler is used to limit the airflow temperature provided by the compressor and a hollow fiber humidifier is considered to transfer water vapour from the fuel cell outlet back into the inlet.

The main components, or functional assemblies of components and their relative functions are described as follows:

Table 6: Air subsystem components and functions

Component (or assembly of components)	Function
Intake including filtering	To deliver air to the compressor intake removing contaminants
Motorised compressor (incl. expander if present)	To compress the incoming air elevating the O2 partial pressure recovering energy from the exhausts
Charge air cooler	To reduce the temperature of the compressed air using coolant
Humidification system	To increase the incoming air humidity level
Exhausts system including condensate extraction	To dispose of the exhausts
Air isolation flap(s)	To isolate the cathode side volume at shut-down allowing the depletion of O2
Ducting	To transfer the flows between the components

3.3.2 Fuel subsystem

The fuel subsystem is designed to produce and maintain a flow of reducing reactants to the anode side of the fuel cell, in a suitable range of temperature, pressure and humidity.

The fuel system is often a closed-loop system, at least in steady state conditions, and the most practical way to generate a humidified fuel stream is a localised recycle around the fuel cell stack. Such recycle can be active, if an externally powered device is used to recompress the outlet mixture, or passive, if the recycle gas is entrained by the expansion of the fresh fuel in an ejector.

The more complex active systems offering greater operational flexibility are often preferred in larger size modules while the simplicity of passive system makes them more desirable for smaller modules.

Due to the large partial pressure difference across the membrane, nitrogen and other inert gases can leak over time to the anode side, progressively diluting the fuel. A component is then required to perform the function of removing it, often a simple purge valve discharging a fraction of the anode gas.

Finally, depending on fundamental the architecture of the stack, in particular the choice of a counterflow versus a co-flow arrangement, a substantial amount of liquid water can be produced within the loop, and its separation from the gas phase is necessary ahead of its disposal.

Table 7: Fuel subsystem components and functions

Component (or assembly of components)	Function
Fuel isolation valve	To isolate the anode side volume
Anode side pressure control valve	To allow adequate flow into the anode side volume regulating the pressure difference to the cathode side. May perform the function of 3.1
Fuel preheater	To pre-heat the incoming fuel avoiding downstream condensation using coolant
Anode recycle pump/ejector	To improve flow distribution inside the stack avoiding accumulation of inerts. To humidify the incoming fuel flow by mixing it with saturated outlet fuel
Purge valve	To discharge a fraction of the fuel removing inerts from the system. To reduce the anode side pressure regulating the pressure difference to the cathode side
Condensate trap	To separate and discharge condensate from the anode side
Ducting	To transfer the flows between the components

3.3.3 Cooling subsystem

The fuel subsystem is designed to maintain the fuel cell stack and all components in the module within the correct operational temperature range.

Commonly, the cooling system is designed to regulate the inlet temperature of the stack and the temperature rise across it.

The former control is obtained by use of a thermostat valve, operated to mix a flow of cold coolant from a heat sink external to the module with a fraction of the warm coolant from the outlet of the module.

The temperature rise across the stack is controlled by acting on the rotational speed of the coolant pump. Finally, a carefully sized expansion tank is generally used to mitigate the pressurisation caused by the reduction in liquid density as the system warms up. Two specific design constraints are key to the sizing of the expansion tank:

- The need to limit the pressure differential across the bi-polar plates, specifically between coolant and cathode. Such constraint is mostly relevant for carbon composite designs.
- The need to avoid cavitation at the inlet to the pump. The correct size of the expansion tank must be determined so that these two requirements are satisfied in all points of operation.

Table 8: Cooling subsystem components and functions

Component (or assembly of components)	Function
Recycle pump	To control stack temperature rise by regulating the coolant flow
Three-way valve	To internally recycle a fraction of the hot coolant regulating coolant temperature at stack inlet. May be used to isolate the cooling circuit
Pipework	To transfer the flows between the components
De-ioniser	To capture ions released in the coolant avoiding electrical shorts internally to the system. May act on a fraction of the coolant flow in a by-pass line.
Cooling fluid	To transfer heat generated in the stack to a heat sink external to the engine
Expansion Tank	To mitigate the pressurisation of the cooling loop caused by the variations of the coolant density with temperature

3.3.4 Electrical subsystem

The electrical subsystem is designed to transfer the commanded amount of electrical power from the fuel cell stack to the external load and the internal module components.

As discussed, the electrical subsystem is the actuator of the fuel cell module as it regulates the electrical current drawn from the fuel cell stack and consequently determines the point of operation of all other subsystems within the module.

Accurate control of the stack current is then crucial to a robust module capable of prompt dynamic response.

In general, the fuel cell module will interface with an external DC system, often regulated in voltage.

The most common solution to the problem posed by these conflicting requirements is the installation of a DC/DC converter within the module, allowing the operation of the stack in carefully controlled current ramps on the

inner interface while the outer interface can be kept at the desired voltage level defined by the other components connected to the DC bus, commonly batteries.

All main auxiliaries within the module will be powered from the outer side of the DC/DC converter, so that they can be operated while the stack is not loaded, drawing power from the DC bus.

It is envisaged that low voltage system will be present, generally 12 or 24V powering smaller consumers and logical devices, however such system will not be described in the present work.

Table 9: Electrical system components and functions

Component (or assembly of components)	Function
Main DC/DC converter	Converts DC power from the fuel cell stack into a determined voltage and current combination
Motorised compressor controller	Provides variable frequency power to the TC motor allowing for variable speed control
Pump controller	Provides variable frequency power to the pump motor allowing for variable speed control
H2 recycle blower controller (if applicable)	Provides variable frequency power to the hydrogen recycle blower motor allowing for variable speed control
Wiring	To transfer power between the components

3.3.5 Control subsystem

The control subsystem is designed to operate the module, the subsystems and the components within them according to a predefined operational strategy ensuring safety.

Additional functions included may be diagnostics and health monitoring functions.

Generally, a single controller is used to operate a fuel cell module, while the logical architecture may include independent subcontrollers for each subsystems logically coordinated by a master controller.

Table 10: Control subsystem components and functions

Component (or assembly of components)	Function
Cabling	To transfer logical signals to and from the subsystems
Instrumentation and sensoring	To acquire information from the system
Fuel cell control unit	To manage the fuel cell stack (health monitoring and diagnostics may be integrated into a single controller)

3.3.6 Mechanical subsystem

The mechanical subsystem is designed to ensure the mechanical integrity of the system in operation. Although multiple component perform mechanical functions, in general two families of functions can be defined:

Table 11: Mechanical subsystem components and functions

Component (or assembly of components)	Function
Casing and confinement	To confine the fuel cell stack as determined by the safety case
Mounting	To locate and support the components in place

4 Definition of a fuel cell module design

A fuel cell module architecture will be defined for a target electrical power output of approximately 100kW. Such configuration will be modelled, and its transient operation will be described.

4.1 Sizing of the main components

The fuel cell module is designed to be capable of pressurised operation in a turbocharged configuration. A state-of-the-art rating of 2.5 bara is assumed as a requirement for all components.

4.1.1 Fuel cell stack

A detailed definition of the internal geometry of the fuel cell stack is not required for the purpose of the present work. In general, the requirements propagating from the stack towards the subsystems require the definition of the eight interfaces towards the four main subsystems [14] [15].

The definition of the interface to the electrical subsystem requires the choice of the number of series-connected cells, set to 600, as well as the active area in each, set to a typical value of 250 cm^2.

A reference performance for the individual cell needs definition as a function of pressure is assumed as described in figure 13.

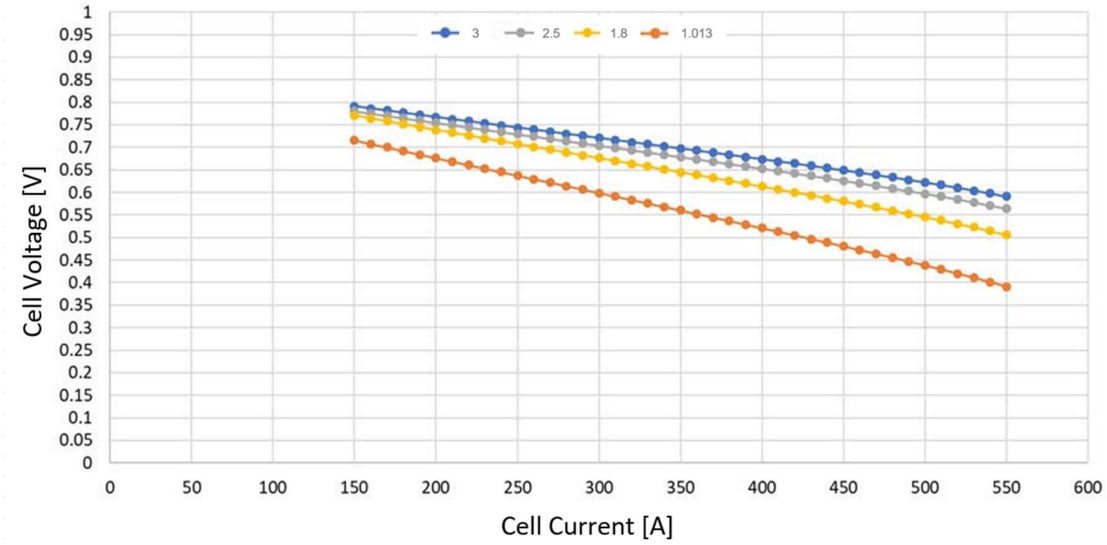

Figure 12: Reference cell performance assumed in the analysis

As explained in chapter 3 such definition of performance cannot alone describe the behaviour of the fuel cell stack in all points of operation, therefore such information will be used as an input to a physical model calculating the operating voltage of an average cell within the stack.

All cells will be assumed with identical performance neglecting the effect of maldistribution of reactants and non-uniform operation in general.

The definition of the air system interfaces in an air-fed system, as the object of the present analysis, is mainly influenced by the choice of the cathode stoichiometry ratio, commonly indicated as lambda.

Such parameter is defined as the ratio between the molar flow of oxygen entering the stack and the amount consumed electrochemically.

The choice of lambda directly influences the performance of the fuel cell stack, the module as a whole, as well as the amount of liquid water produced and the thermal balance of the stack with it.

Specifically, a higher lambda determines a higher partial pressure of oxygen at the cathode with a consequent improvement in cell voltage, performance, and durability [16].

However, even in a turbocharged architecture the air system remains a net consumer of power and its impact on the net power output is greater at higher values of lambda.

Commonly, most fuel cell modules are operated in a range of lambda between 1.5 and 2, with the only exception of evaporatively cooled stacks operating at higher values to enable sufficient cooling.

A typical value of 1.8 will be assumed.

Similarly to lambda, an anode stoichiometry parameter can be defined as the ratio between the hydrogen flow at stack inlet and the amount consumed electrochemically. Given, at steady state, the fuel subsystem as a whole is dead-ended such value is determined locally at the stack interfaces by the amount of stack off-gas recycled back to the inlet.

A greater recycled flow corresponds to a higher anode stoichiometry locally at the stack interfaces, while the hydrogen consumption remains constant as purely dependent on the stack current.

A lower limit to anode stoichiometry is normally sufficient as the main purpose of anode recycle is to guarantee a minimal flow to the stack required for a correct internal gas distribution and to recycle an amount of water vapour sufficient for anode side humidification.

A defined upper limit for anode stoichiometry is in practice not necessary as the consequences of the resulting hydrogen dilution on performance are often negligible.

For the purpose of the present analysis a minimum value of 2 is set as target for anode stoichiometry.

Finally, the design point of the fuel cell module is defined as corresponding to a 300A current drawn from the fuel cell stack, as a conservative choice for a high efficiency design, still aimed at a target of power output greater than 100kW.

4.1.2 Air subsystem

As a direct consequence of the sizing of the fuel cell stack and the choice of lambda an air massflow requirement can be determined, translating into approximately 120 g/s of compressed air at the aforementioned pressure of 2.5 bara.

Among the turbocharging units specifically developed for fuel cell modules the EMTCT-120k unit from Fischer correctly fits the fundamental requirements and it will be used in the analysis.

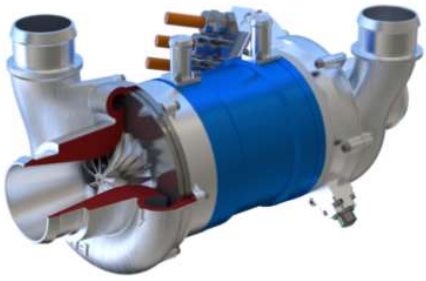

Figure 13: The Fischer EMTCT-120K [17]

Such turbocharger consists of a radial centrifugal compressor coupled to a radial turbine via an electrically motorised shaft. Oil-free groove bearings are used, relying on channels carved in the body of the shaft to create an air film supporting the shaft while spinning, thus avoiding contact between the metallic parts.

Such solution avoids the risk of oil contamination in the incoming air to the stack.

The permanent magnet synchronous machine driving the shaft is installed between compressor and turbine and it is wired to a variable-frequency inverter required to operate the device, interfacing to an HV3 520-750 V DC bus.

The inverter operating frequency in operation is proportional to the rotational speed of the machine allowing for its accurate control.

Finally, liquid cooling is required both for the electrical motor and the inverter, however due to the very limited cooling power requirement such constraint is not part of the analysis carried out.

Detailed performance maps for compressor and expander are not provided publicly by Fischer, therefore compatible maps for machines of similar size available in literature will be used to define the model, maintaining alignment with the incomplete information published[18].

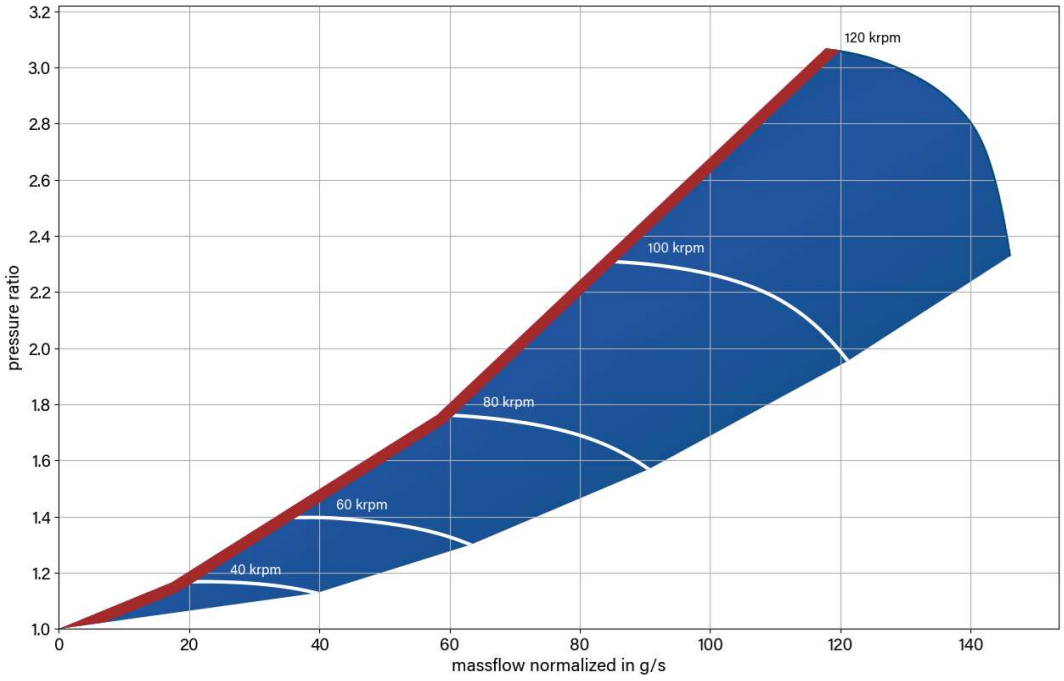

Figure 14: Reference compressor map published by Fischer

The humidifier was sized as a hollow fiber design, as opposed to the promising but still less mature membrane technology. Hollow fibers, allow for the selective flow of water from the lower pressure fuel cell outlet towards the incoming dryer air. Such flow, fundamentally driven by the difference in partial pressure of water vapour between the two streams, allow the humidification of the incoming airflow while avoiding the dilution with nitrogen that a simple gas recycle would have implied.

Figure 15: Example of a hollow fiber air humidifier: Fumatech 100N [19]

To achieve a correct matching with the fuel cell stack and the turbocharger a customised design has been assumed in the modelling.

The separation and extraction of the condensate water is assumed to take place at the outlet from the stack.

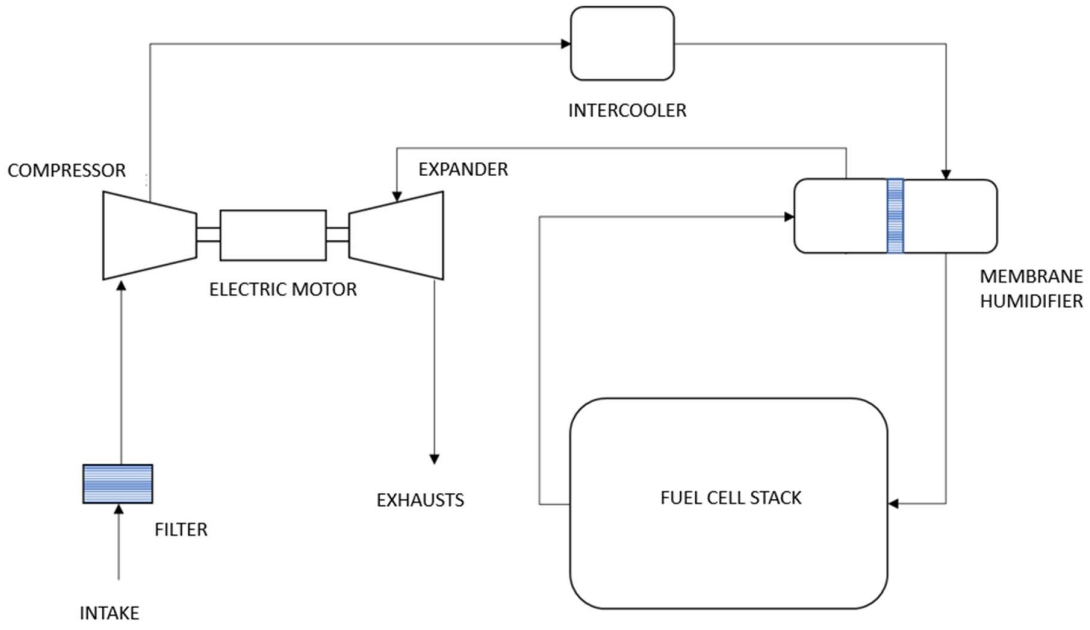

Figure 16: Main components within the air system and their relative location

4.1.3 Fuel subsystem

The system is designed with a passive anode recycle system. An ejector driven by the inlet hydrogen pressure was chosen to entrain the off-gas from the fuel cell as opposed to a power-consuming active recycle device.

A 0-D model of the ejector [20] was used to determine the basic sizing of the fundamental flow sections within the ejector and to produce performance maps required as inputs into the main performance model.

The ejector design was optimized for the reference conditions shown in Table 12, based on a target dry gas composition on the secondary inlet.

Table 12: Reference point for the sizing of the anode ejector

Primary Pressure [bara]	2.8
Primary Temperature [°C]	25
Primary Flow [g/s]	1.88
Primary H2 % (vol)	100%
Secondary pressure [bara]	2.5
Secondary Temperature [°C]	70
Secondary H2 % (vol)	70%
Secondary N2 % (vol)	30%
Target recycle ratio (vol)	2

Similarly to the cathode system the separation and extraction of the condensate water is assumed to take place at the outlet from the stack.

4.1.4 Cooling Subsystem

A generic set of performance curves was used to define the performance of the coolant pump in the model.

The coolant side of the intercooler has been modelled with a simplified approach as a heat addition to the liquid.

The coolant is assumed to be a mixture of glycol ethylene and demineralised water, at 50% in volume, as typical for most fuel cell systems [22].

The thermostat valve (TV), a three-way valve, is represented as the combination of two two-way valves operated in conjunction, with fractional openings constrained to be complementary to 100%.

4.1.5 Electrical Subsystem

The representation of the electrical subsystem is very basic, as the accurate representation of such subsystem in the range of time constants typical of power electronics is not of interest for its lack of impact on the other subsystems.

In the model, the internal circuit only is represented, on the stack side of the DC/DC converter and the external interface to the platform is calculated assuming a constant 98% efficiency in the power conversion to the DC BUS voltage.

A simple current source is used to apply the electrical interface to the stack and it is operated according to fig. 20.

4.2 The modelling environment

The model for the fuel cell module was built using a GT-Suite, a commercially available modelling software produced by Gamma Technologies [21].

GT-Suite includes an extensive library of components for the transient modelling of internal combustion engines and power systems in general.

Ducts, control valves, compressor and expanders, liquid cooling components are available within the GT-Suite libraries together with some more specific fuel cell system components.

Among them a detailed fuel cell stack component allows not only to transiently calculate the operating conditions based on a physical model of the electrochemical performance, but it also allows to match a target performance within the range of variation for the sizing parameters. Such component models the behaviour of a fuel cell stack with sufficient accuracy for the objectives of this work[22] [23] [24].

Hollow-fiber humidifiers are also available in the components' library, freely sizeable to match the desired water transfer performance [25].

Overall, GT-Suite provides a robust, reliable and adequately accurate transient modelling environment for the purpose of the present work; the solver is highly customisable in methods and accuracy while it offers the opportunities for co-simulation in combination with several modelling tools. Nonetheless, the existing components' library is extensive and covers all the components required.

4.2.1 Main modelling assumptions

A basic control system was defined to regulate the main performance parameters transiently throughout the transitions [26] [27].

The airflow through the cathode side of the stack was regulated to maintain a value of lambda as close as possible to 1.8, acting on the rotational speed of the motorised turbocharger. Such basic control logic relies on a simple dependency of rotational speed to stack current, implemented in the model as a lookup table.

Similarly, a lookup table was used to determine the position of the humidifier by-pass valve with the target to maintain the relative humidity at the inlet to the cathode in an acceptable 65%-75% range in all points of operation.

The thermostat valve recycling warm coolant to regulate the temperature at the inlet to the stack is operated based on a closed loop control, while the flow through the stack is regulated again with an open loop link to stack current via a third lookup table [28] [29] [30].

Finally, a PID controller regulates the incoming hydrogen pressure to maintain a positive pressure difference of 100 mbar between the anode and the cathode, a common requirement for the operation of PEM stacks. In the present version of the model, only the proportional component is enabled.

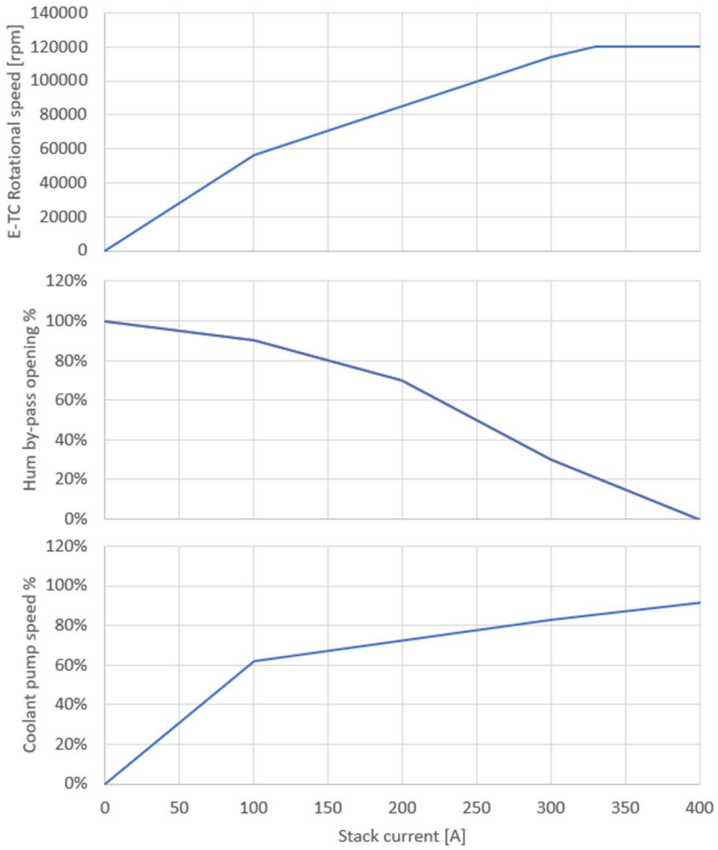

Figure 17: Lookup tables regulating E-TC speed, By-pass valve opening and coolant pump speed

The crossover of Nitrogen [31] [32] from the cathode to the anode side, driven by the different partial pressure differences across the membrane was set as 0.001 moles/bar while a purge valve was sized with a full opening flow section of 2.5 mm^2.

A purge frequency of 30s was initially selected, with 1s opening time for the purge valve in each cycle. Such purge frequency was kept constant throughout operation and the resulting nitrogen partial pressure at anode outlet was monitored to assess the viability of such strategy.

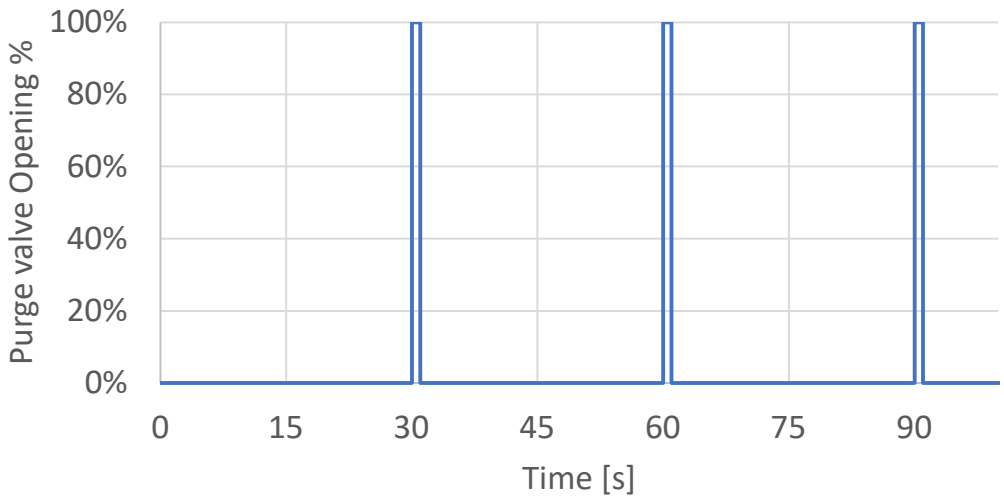

Figure 18: Operational schedule of the purge valve

Such basic set of control functions constitutes the strict minimum required to operate the model transiently. It is however envisaged that a more advanced approach would be required to ensure better operational flexibility and faster dynamics. Such activity is not covered in the present work.

4.2.2 The case study

The model was assembled and exercised to represent the operation of the fuel cell module at design point, defined as 300A drawn from the stack and its transition to and from a low power point defined as 100A.

Such load profile is consistent with the operation of one or multiple fuel cell modules in combination with an electrical battery.

In such configuration, often referred to as “range extender” the immediate response of the system is taken care of by the battery while the fuel cell module transitions to a higher load point along defined load ramps.

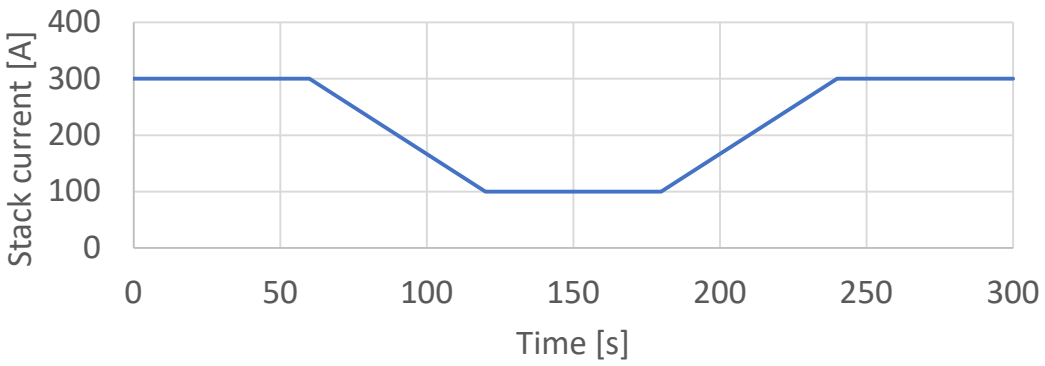

Figure 19: Stack load profile

Such load profile, shown in fig. 20 will be used as a case study in the present work. At the beginning of the simulation the model is taken to a steady state.

4.2.3 Model overview

The model appearance in the graphical user interface of GT-Suite is shown in fig 21.

Streams in each of the main subsystems are represented in a dedicated colour, green for the air subsystem, red for the fuel, blue for the coolant and yellow for the electrical.

Logical signals are represented as thinner blue lines.

The lower left part of the diagram describes the air system with its main components, with the individually shown compressor, turbine and motorised shaft constituting the E-TC.

The hollow-fiber humidifier was iteratively sized as an assembly of 2400 250mm-long flow tubes made of Nafion.

The charge air cooler was sized conservatively to achieve a temperature difference of 10°C between the air outlet and the coolant at design point, resulting in a UA of 0.18 kW/K.

All ducts connecting the components are represented with assumptions made on size and volumes, so that pressure drops can be estimated.

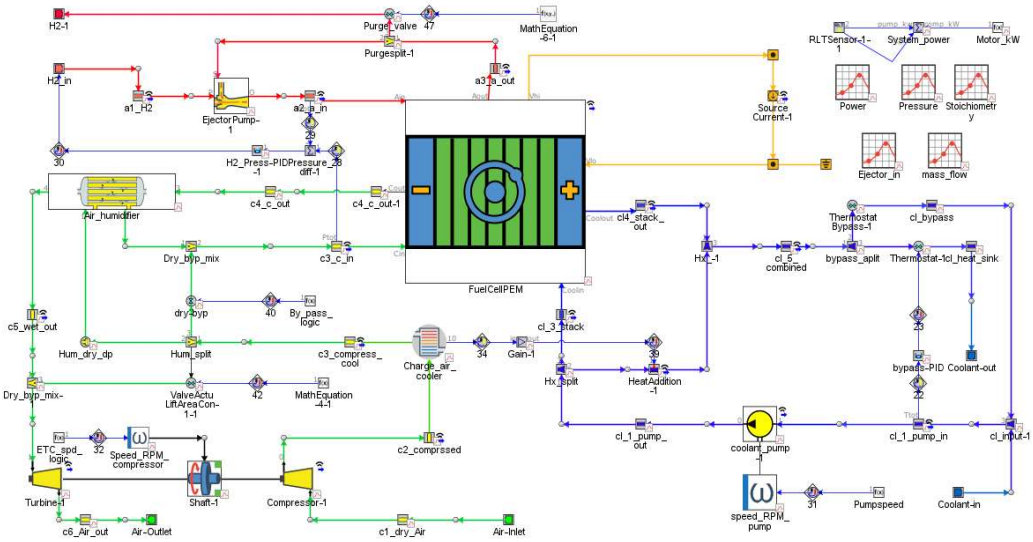

Figure 20: Model overview in GT-Suite

Similarly, the upper left section represents the fuel subsystem with a variable pressure inlet interface for the fresh fuel representing a flow section downstream of the pressure regulating valve.

The electrical subsystem on the upper right section is simply represented as a DC interface, as any representation of a DC/DC power converter in a thermodynamic model operating well above its switching frequencies would be of very limited value. Nonetheless, a power conversion efficiency of 98% is assumed for such component in all points of operation.

Finally, the lower right section represents the cooling system, neglecting the external heat sink, typically a liquid-to-liquid heat exchanger in a marine

application, as such component, specific to each application, is not considered part of the fuel cell module.

The coolant is assumed to be entering the module boundary at a constant temperature of 68C: for the case study under investigation it is assumed that the seawater flow can be regulated to achieve a constant coolant return temperature to the modules.

As a consequence the operation of the thermostat valve (TV) included in the model, and represented as the combination of two two-way valves operated in conjunction, is not necessary.

An extension of the scope of analysis including multiple modules connected to a single WSHE would be required to optimise the operation of TV in the normal operation state of the module. This is outside of the scope of the present work.

5 Analysis of the module operation

The calculated operating conditions of the module and its subsystems will be shown in the case study defined in section 4.2.2.

5.1 Performance of the fuel cell stack

The transition to the lower power point of operation determines an increase in the operating voltage, as expected [33].

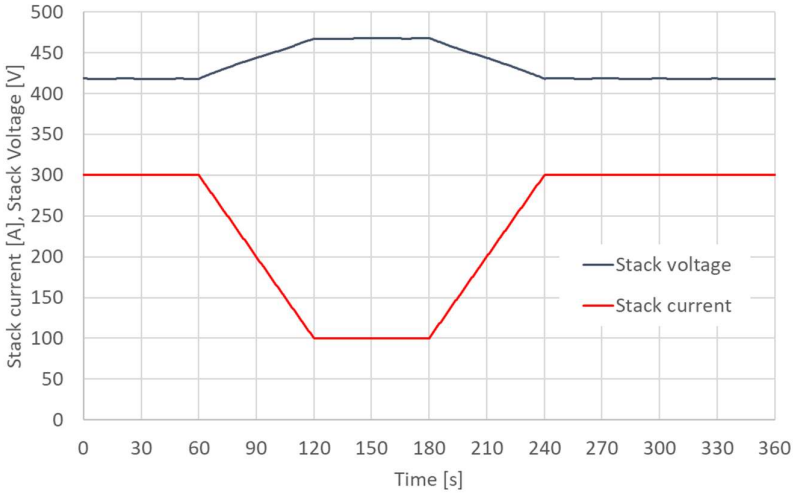

Figure 21: Stack voltage

Such increase in voltage determines a proportional increase in the LHV efficiency of the stack, where.

$$\eta = \frac{IV}{\dot{m}H_2 \times LHV} \quad (2)$$

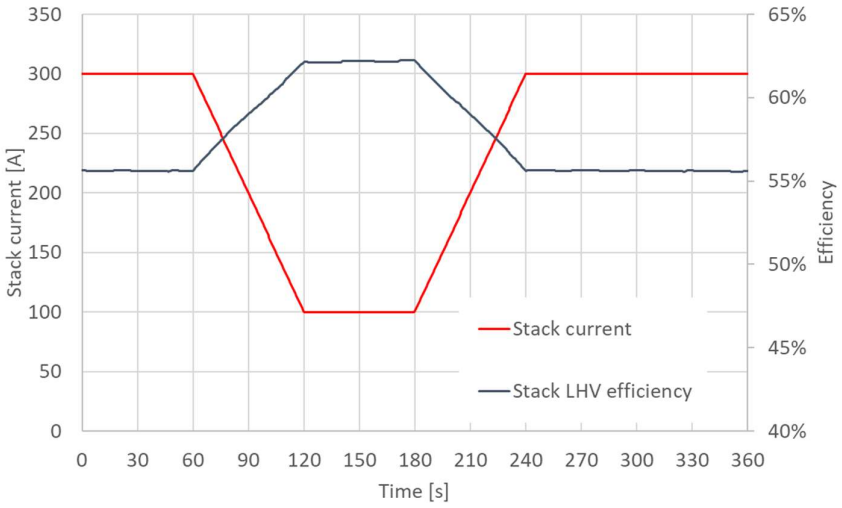

Figure 22: Stack LHV Efficiency

Both the voltage trace in fig. 22 and the resulting efficiency trace in fig. 23 present visible non-uniformities suggesting that the module never actually reaches a true steady state. This is consistent with the hypotheses made on anode-loop operation, specifically on the intermittent purge strategy, and such phenomena will be described in better detail later within the present work.

5.2 Fuel Subsystem Behaviour

As a consequence of the opening strategy of the purge valve described in fig. 19, the module performs cyclic discharges of the anode gas mixture [34]. The massflow discharged is, as expected, larger at higher loads due to the higher pressure upstream of the purge valve.

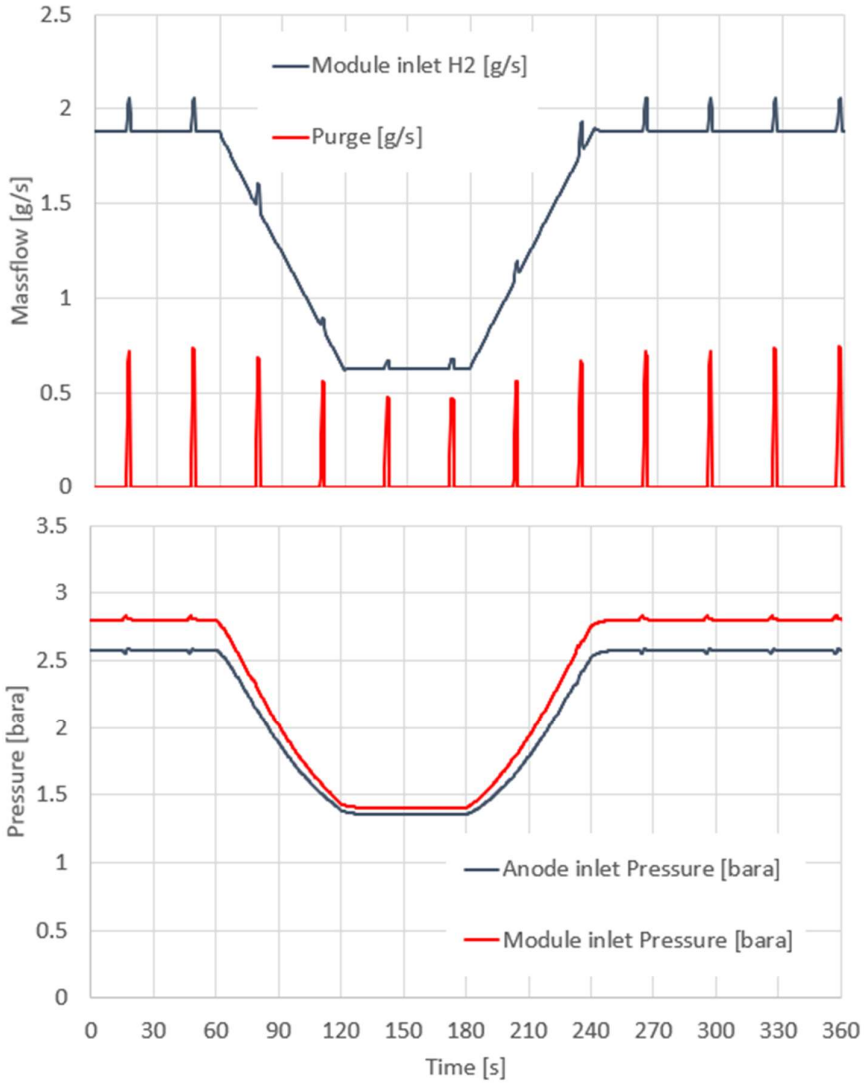

Figure 23: Purge flow and effect on pressure

Fresh hydrogen is then fed into the module as the anode pressure control function responds to the depressurisation of the anode side with an increase in module inlet pressure.

The desired effect of the purge cycle is a reduction in the partial pressure of Nitrogen in the anode subsystem. Such effect is visible in fig. 25 describing the behaviour of the dry gas composition at the anode outlet of the fuel cell stack.

At steady state and full-load the adopted purge strategy maintains the fraction of hydrogen well above 70%.

On the other hand, at low load the nitrogen dilution reaches 50%, on the lower end of the commonly considered acceptable range. The descending ramp to the low load point is the most critical phase because the depressurisation of the system limits the incoming hydrogen flow as the system indirectly regulates the incoming fuel flow while controlling the anode side pressure.

Finally, the ramp to full load successfully returns the nitrogen dilution levels under 30%. Noticeably the ascending ramp terminates at the lowest value of nitrogen dilution in the simulation as the anode volume is re-pressurised with additional fresh hydrogen.

The loss of hydrogen associated to purging of the anode loop is calculated to be in the order of 0.1% of the incoming fuel.

Finally, a drop in anode stoichiometry is visible at the low load point of operation, despite a small increase in recycle ratio. This is a direct consequence of the increased nitrogen dilution as a smaller fraction of hydrogen is present in the recycled gas flow. Nonetheless, anode stoichiometry remains above 1.5 throughout operation.

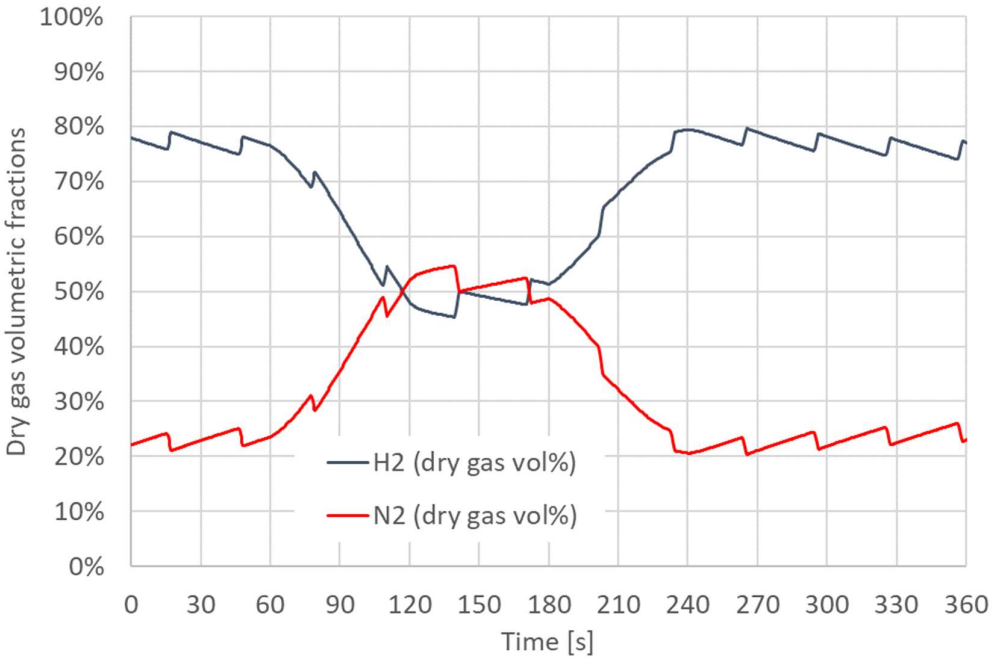

Figure 24: Effect of purge cycles on anode outlet gas composition

A disadvantage of the chosen passive recycle solution is the inability to mitigate such effect by regulating an active device to increase the recycle ratio.

Nonetheless, a more aggressive purge strategy at low loads could be used to raise anode stoichiometry by reducing dilution, with a small impact on performance.

Multiple hybrid configurations between passive and active have been proposed to mitigate the operational limitations of a simple passive system, relying on multiple ejectors, or a combination of ejectors and active blowers. The viability of each solution is dependent on the module size, operational requirements and suitability to the application and it cannot be assessed independently.

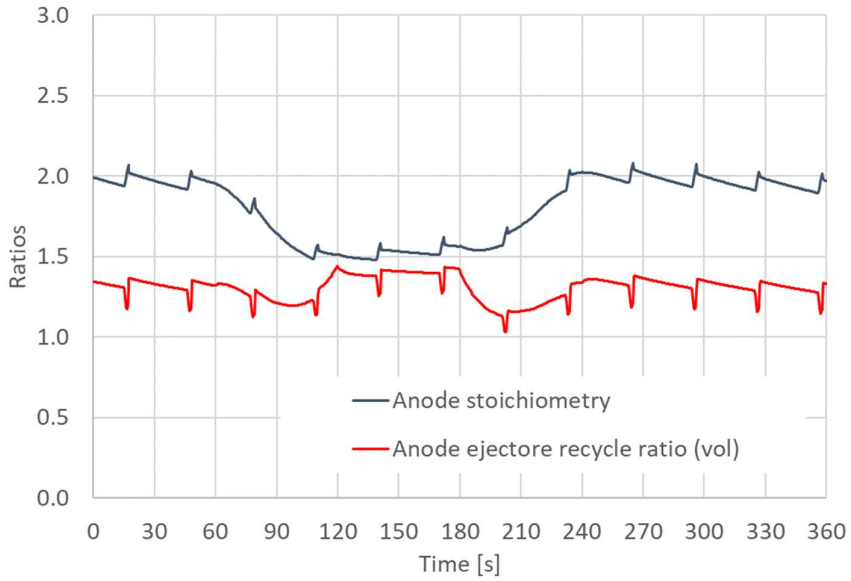

Figure 25: Anode stoichoimetry

5.3 Air Subsystem Behaviour

The air subsystem determines the system's pressure directly on the cathode side, and indirectly on the anode side as the two pressures are tied in operation by the requirement to limit the pressure difference across stack the membrane.

The air humidification requirements at the inlet to the stack are set in

$$RH = \frac{P \times x_{H2O}}{P_{sat}} \tag{3}$$

terms of relative humidity and operating pressure is inversely proportional to the required volumetric fraction of water vapour for a given target relative humidity. The system analysed is not designed to actively regulate operating pressure in operation, therefore it transitions between load points on a fixed load line on the compressor map, for a given set of boundary conditions.

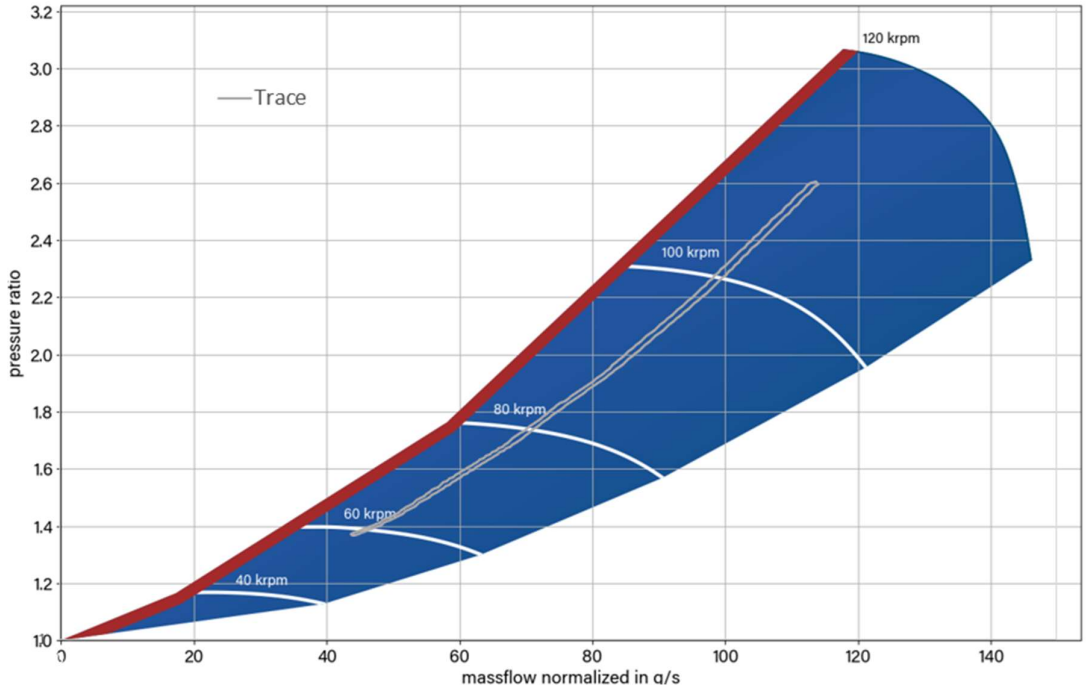

Figure 26: Trace on the compressor map (see fig.15)

In the case study under investigation, the trace on the compressor map, shown in fig. 27, shows a consistent behaviour for descending and ascending ramps, with limited hysteresis as the descending ramp is marginally closer to the surge line due to the delay in the depressurisation of the volumes within the air subsystem.

As the E-TC rotational speed varies because of the variation in stack current via the control function described in fig. 18 the air subsystem depressurises as shown in fig. 28.

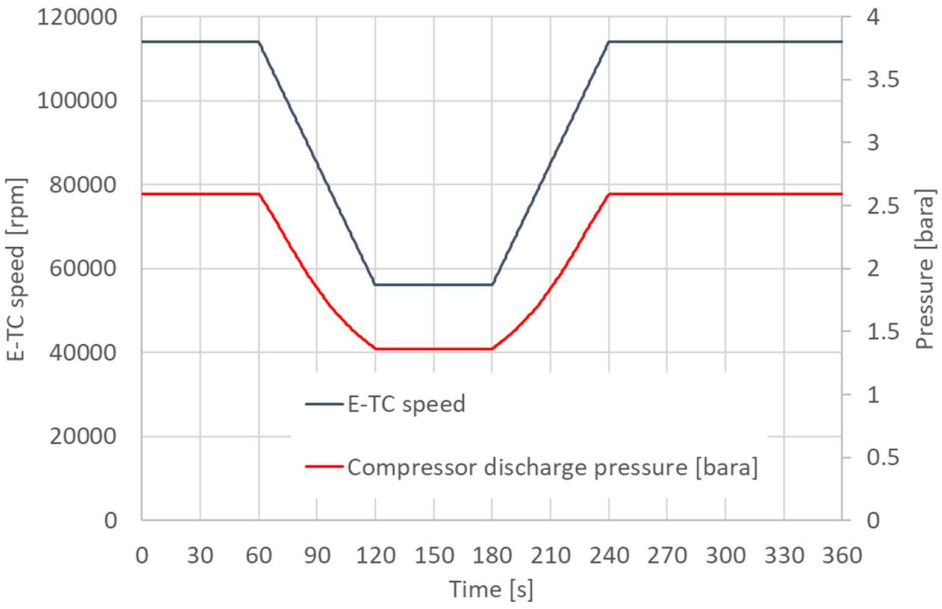

Figure 27: Depressurisation of the air subsystem

On the E-TC shaft, the power provided by the electric motor is estimated to exceed that of the turbine at full load while the contributions are similar at low load. Bearing losses have been assumed as 1% of the compressor power, while power conversion efficiencies in the DC/AC inverter and the permanent magnet synchronous machine have been assumed as 98% and 96% respectively.

The adiabatic isentropic efficiencies of both compressor and turbine remain above 70% in all points of operation.

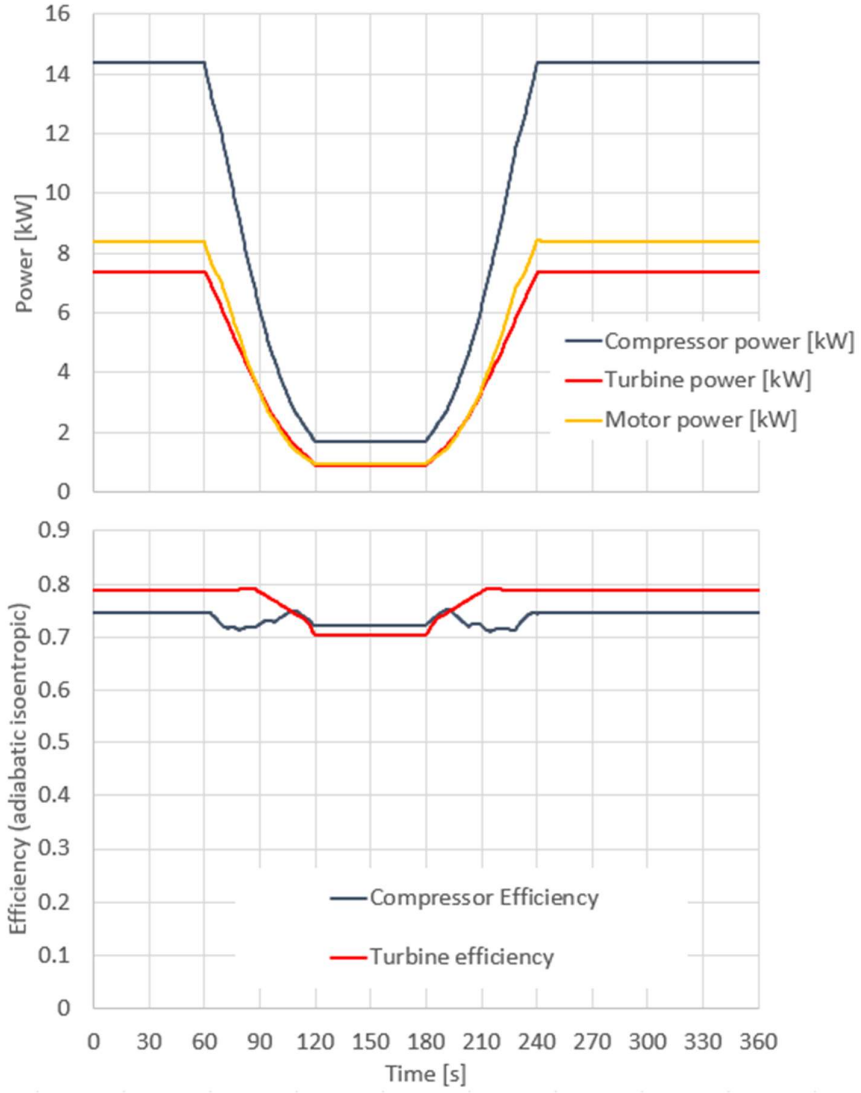

Figure 28: E-TC Performance

Even without a closed loop correction the simple feed forward control algorithm implemented in the model is able to maintain cathode stoichiometry (lambda) close to the steady state target of 1.8, with a minimum value of 1.73 in the final section of the ascending ramp.

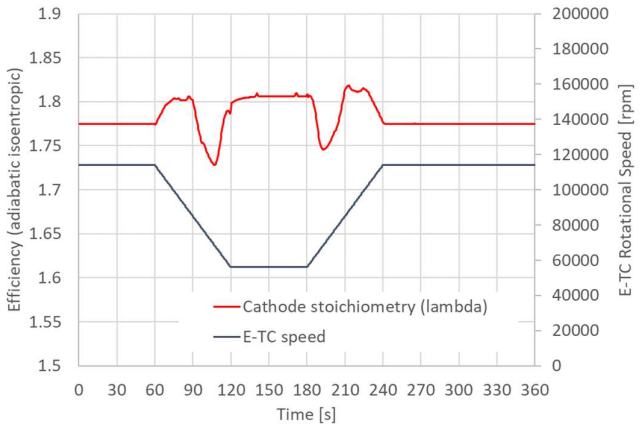

Figure 29: Cathode stoichiometry (lambda)

At the inlet to the stack, the target of a relative humidity in the 65%-75% range is achieved throughout the case study.

As the current drawn from the stack is reduced the by-pass valve opens throughout the descending ramp as the water transfer rate required to achieve the target relative humidity is reduced, due to the airflow reduction.

Transiently during the load ramps the relative humidity reaches a local minimum value eventually returning to a higher value as the system reaches steady state.

The open loop control function regulating the fractional opening of the by-pass valve achieves a correct steady state condition but it cannot avoid such deviation during the ascending and descending ramps.

Such deviation is nonetheless minimal at the ramprates used in the case study, and well within the acceptable range.

A closed loop control would be required to achieve a more accurate control, hence enabling faster ramprates, however a direct measurement of the relative humidity is often impractical for lack of cost-effective reliable sensors and even a more advanced control would have most likely to rely on indirect measurements.

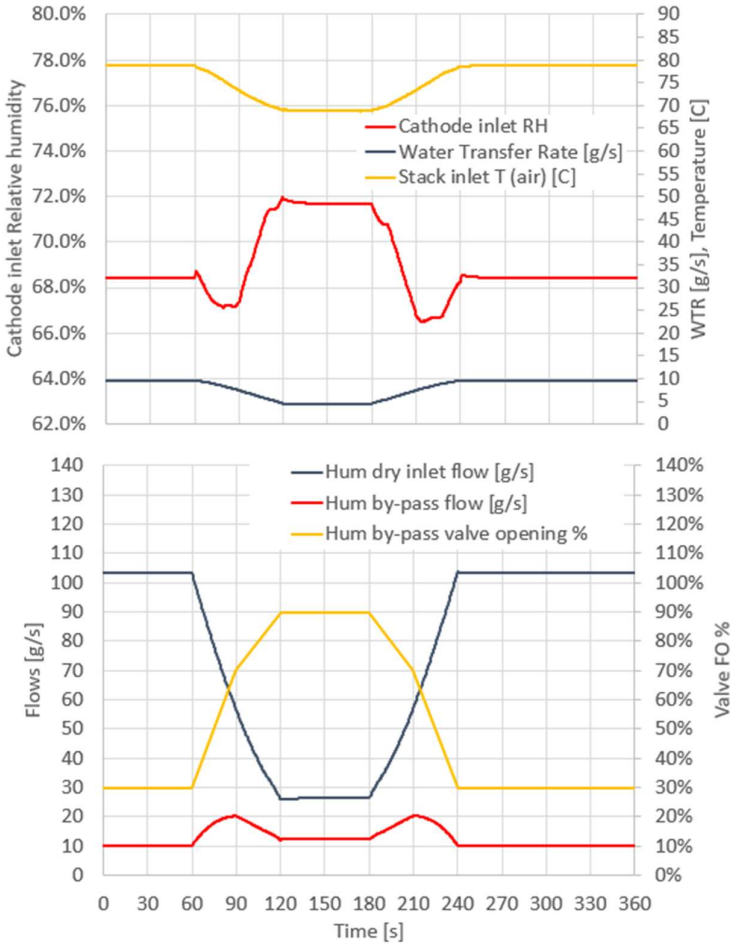

Figure 30: Relative humidity control and humidifier by-pass valve

The system by-pass valve, included in the model, allows the operation of the system at reduced pressure by diverting an airflow from the humidifier dry inlet towards the turbine. Its operation can move the operating point of the compressor on the map increasing the distance to the surge line. However, such action is not necessary in the present case study as the module operates well within the allowed operating envelope throughout (fig. 27).

5.4 Cooling Subsystem Behaviour

The main objective of the cooling subsystem is to maintain the temperature rise across the fuel cell stack within a limit commonly set at 10°C.

In marine applications the cooling loop is closed by a liquid to liquid heat exchanger (WSHE) fed on the external side with seawater.

Cooling capacity is abundant in these applications as the surface seawater temperature can rarely reach 30°C, while the target coolant inlet temperature for the module is set as 68°C.

The control function described in fig 18 determines a deceleration of the coolant pump as the descending load ramp progresses towards the low load point.

The effect is an effective control of the temperature rise across the fuel cell stack, as shown in fig. 32, with a deviation of the stack outlet temperature of approximately one degree centigrade.

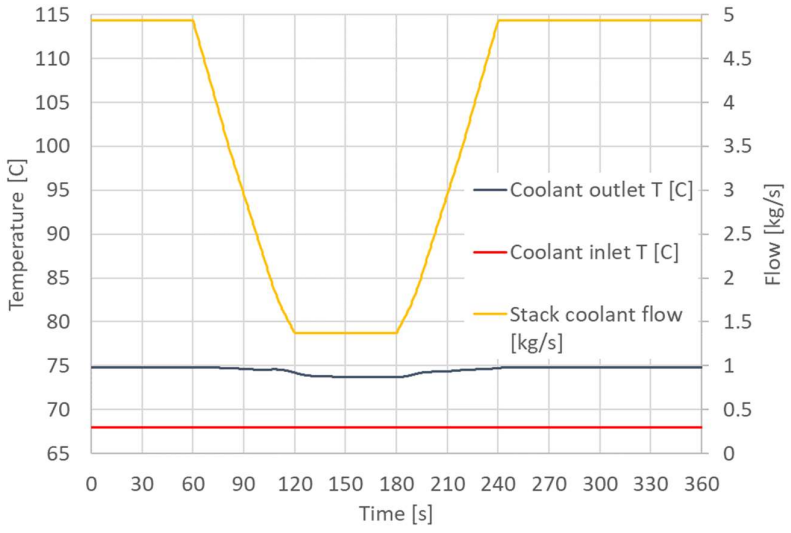

Figure 31: Stack coolant temperatures

The trace on the operating map of the pump is shown in fig 33.

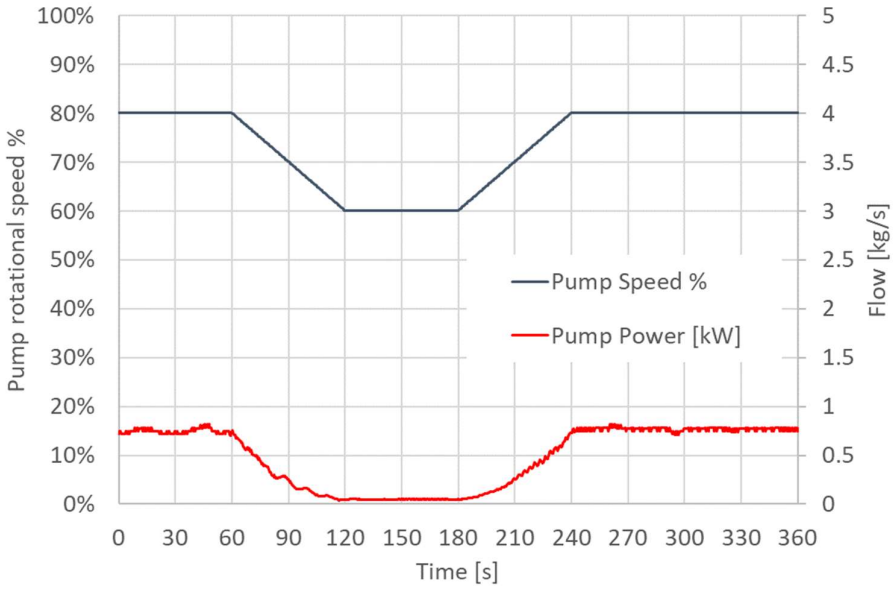

Figure 32: Coolant pump flow and trace

5.5 Module Performance

The fuel cell model performance varies during the case study as described in fig. 34. As typical of fuel cell systems the increase in cell voltage described in fig. 23 leads to an increase in the net module efficiency, still calculated on LHV, approaching 60% at the low load point.

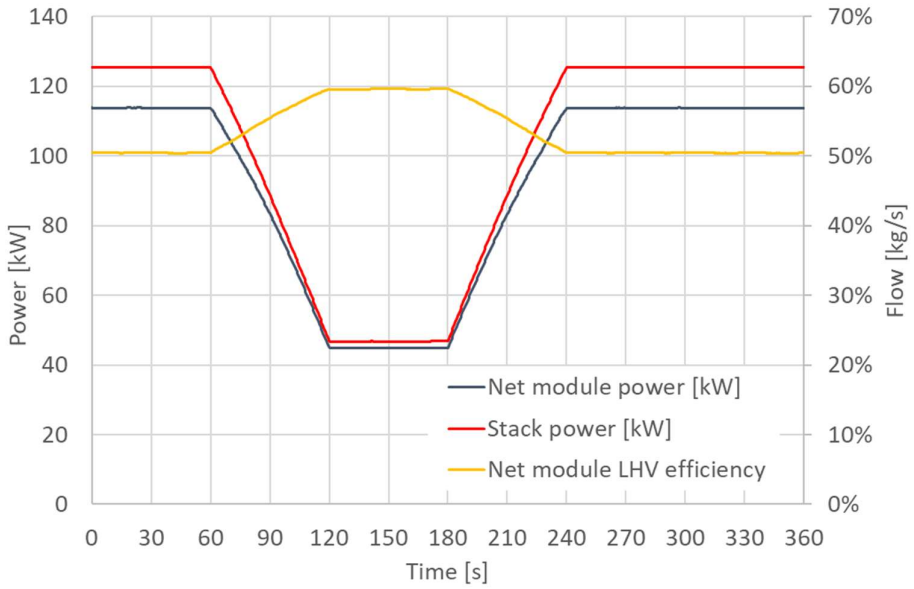

Figure 33: Stack and module performance

The internal consumptions, including DC/DC power conversion and the two main power consumers, E-TC and coolant pump negatively account for about 10kWe at design point power, but their impact is reduced to less than 2kWe at the low load point.

In general, the module performance reflects the design intent to achieve a very high efficiency in all points of operation, relying on a relatively generous stack sizing, as a way to enable longer range operation in marine application.

6 Conclusions

The work presented focused on the definition of a fuel module architecture suitable for integration into a marine propulsion platform. The fundamental design choices focused on achieving a higher power conversion efficiency as opposed to a typical automotive design, simultaneously constrained in volumetric power density.

The fuel cell stack was sized to achieve such purpose.

The subsystems and their functions were defined and the components within them were defined and sized to match.

A transient-capable model representing each component and the subsystems was developed in the commercial tool GT-Suite.

Appropriate assumptions were made to align the model components to the defined characteristics.

A basic control system was defined for the module enabling operation in off-design conditions.

A case study was defined to represent the behaviour of one or many fuel cell modules coupled to a battery storage within a marine propulsion system.

The performance of the module as well as the behaviour of each subsystem was evaluated and described, proving not only the desired excellent performance, but also the ability to transition between the load points.

The issue of anode side dilution with Nitrogen was addressed and the viability of the proposed operating strategy was confirmed.

Overall, the proposed design architecture was demonstrated to achieve the desired performance and operational characteristics.

While the performance of the proposed architecture can potentially match a wide range of vessel sizes, it is envisaged that a scale-up in module power output would be required for applications in the multi-MW power range.

With today's technological limit of about 500 cm^2 cell active area, and the performance advantages obtainable by operating with larger scale turbocharging systems and auxiliaries, 250 kW is a realistic short term upper limit for a high performance fuel cell module.

In conclusion, the proposed architecture suits effectively a modular redundant sub-MW propulsion system.

6.1 Opportunities for further improvement

The analysis work focused exclusively on the normal operation state of the system, and a simple controls architecture was defined to enable transitions between the operating points.

A more robust and advanced control system would be required to perform faster load ramps, ensure optimal operation in a wide range of ambient conditions as well as managing the start-up and shut-down phases of operation.

It is envisaged that closed loop controls fed with sensor data would be required to achieve such capabilities. Nonetheless, the existing open loop correlations would be implementable as feed-forward corrections.

Optimisation of the anode loop purging sequence could be carried out as a compromise between efficiency and dynamic capabilities. In practice the negative impact on performance due to the more frequent purging could be offset by the higher available fuel buffer enabling faster load ramps. These balance between these conflicting requirements can only be sorted within the target requirements for the whole propulsion system.

While the study focused on a typical 100kWe size module, today's state-of-the-art, in many marine applications a larger module size would be beneficial, as the total installed power could exceed several MW.

Finally, a larger size design [35] could offer opportunities in terms of more efficient components, rated to higher pressure. Thermal recuperation across the turbocharger. From compressor outlet to turbine inlet, can be more easily cost effective at larger scale, further reducing the energy cost of the air compression equipment.

Bibliography

[1] European Maritime Transport Environmental Report, EMSA, 2021.

[2] Energy Transition outlook - Executive Summary, DNV, 2021.

[3] Maritime Forecast to 2050, DNV, 2021.

[4] Vaferi M, Pazouki K., Van Klink A., « Declines in EROI of Main Fuels and the Implications on Developing LNG as a Marine Fuel », Int. J. of Marine Science and Engineering, 8(9)-719 (2020).

[5] "Pioneering gas turbine-electric system in cruise ships: A performance update" https://lloydslist.com/LL1133876/IEA-estimates-zero-emission-shipping-to-cost-$6trn Sanneman, B.N.,. Marine Technology and Sname News, 41(4): 161-166

[6] ISO 14687:2019 Hydrogen fuel quality, https://www.iso.org/standard/69539.html

[7] L. Mantelli, M.L. Ferrari, A. Traverso, Dynamics and control of a turbocharged solid oxide fuel cell system, Applied Thermal Engineering, 191 (2021), 116862. https://doi.org/10.1016/j.applthermaleng.2021.116862

[8] Doug Woodyard, "Marine Diesel Engines and Gas Turbines, 2004, Elsevier, ISBN 0 7506 5846 0

[9] Geertsma RD, Negenborn RR, Visser K, Hopman JJ. Design and control of hybrid power and propulsion systems for smart ships: a review of developments. Appl Energy 2017;194:30–54. https://doi.org/10.1016/j.apenergy.2017.02.060.

[10] K. Machajabc, J. Kupeckiabd, Z. Malechac, A.W. Morawskie, M. Skrzypkiewiczab, M. Stanclikc, M. Chorowskic, "Ammonia as a potential marine fuel: A review", Energy Strategy Reviews, 44-100926 (2022), https://doi.org/10.1016/j.esr.2022.100926 .

[11] A.G. Elkafas, M. Rivarolo, E. Gadducci, L. Magistri, A.F. Massardo, "Fuel Cell Systems for Maritime: A Review of Research Development, Commercial Products, Applications,and Perspectives", https://doi.org/10.3390/pr11010097.

[12] Shuai Ma , Meng Lin, Tzu-En Lin, Tian Lan, Xun Liao, F. Maréchal, J. Van Herle, Y. Yang, C. Dong Fuel cell-battery hybrid systems for mobility and off-grid applications: a review. Renew Sustain Energy Rev July 2020;135:2021. https://doi.org/ 10.1016/j.rser.2020.110119.

[13] Cellcentric presents latest generation of its fuel-cell technology: https://cellcentric.net/en/cellcentric-iaa-transportation-2022/ 13 Sep 2022

[14] Nuchturee C, Li T, Xia H. Energy efficiency of integrated electric propulsion for ships – a review. Renew Sustain Energy Rev 2018;134:2020. https://doi.org/10.1016/j.rser.2020.110145.

[15] Barbir F, Gomez T, Efficiency and economics of proton exchange membrane (PEM) fuel cells, Int. Journal of Hydrogen Energy, 22 (1997), 1027-1037.

[16] W. Schmittinger, A. Vahidi, E. Bellisio A review of the main parameters influencing long-term performance and durability of PEM fuel cells, Journal of Power Sources 180 (2008) 1–14. doi:10.1016/j.jpowsour.2008.01.070.

[17] Fischer Fuel Cell Turbocharger EMTCT-120k: https://www.fischer-fuelcell-compressor.com/fileadmin/user_upload/02_FFCC/DOKUMENTE/EMTC_T_-120k_Gen4_EN.pdf

[18] Garrett Performance Catalog v9: https://www.garrettmotion.com/wp-content/uploads/2022/07/Garrett_Performance_Catalog_Volume-9_2022.pdf

[19] Fumatech humidifier 100N https://www.fumatech.com/en/products/humidifier-modules-ecomate

[20] D. Bernardi, M. Bozzolo, F. Marsano, O. Tarnowski, Ejectors Design in the Rolls-Royce 1MW Hybrid System, GT2005-68085, ASME Turbo Expo 2005: Power for Land, Sea, and Air

[21] Gamma Technologies GT-Suite: https://www.gtisoft.com/gt-suite/

[22] Springer TE, Zawodzinski TA, Gottesfeld S, Polymer Electrolyte fuel cell model, Journal of The Electrochemical Society 138, (1991), 2334-2342.

[23] R.F. Mann, J.C. Amphlett, M.I. Hooper, H.M. Jensen, B.Peppley, P.R. Roberge, Development and application of a generalised steady state electrochemical model for PEM fuel cell, Journal of Power Sources, 86 (2000) 173-180.

[24] Amphlett JC, Mann RF, Peppley BA, Roberge PR, Rodrigues A, A model predicting transient responsis of proton exchange membrane fuel cells, 61 (1996), 183-188.

[25] Water transport analysis of hollow fiber membrane humidifier module using response surface method: Thermal Science and Engineering Progress, Volume 49, March 2024, 102453

[26] J.C. Gómez, M. Serra, A. Husar, Controller design for polymer electrolyte membrane fuel cell systems for automotive applications, Int J of Hydrogen Energy, 46 (2021), 23263-23278. https://doi.org/10.1016/j.ijhydene.2021.04.136

[27] M. Cavo, L. Mantelli, S. Crosa, M. Bozzolo, L. Magistri, Modelling and Control System Development of a Turbocharged Proton-Exchange Membrane Fuel Cell System, ASME GT2023-102571

[28] A. Amirfazli, S. Asghari, M. Koosha, Mathematical modeling and simulation of thermal management in polymer electrolyte membrane fuel cell stacks, M., Journal of Power Sources, 268 (2014), 533-545.

[29] K. Ou, Y. Wang, Z. Li, Y. Shen, D. Xuan, Feedforward fuzzy-PID control for air flow regulation of PEM fuel cell system, Int J of Hydrogen Energy, 40 (2015), 11686-11695. https://doi.org/10.1016/j.ijhydene.2015.04.080

[30] M. Bozzolo, F. Caratozzolo, D. Silveira Erel, A.Traverso, US10622650B2 System and method for fuel cell stack temperature control, US Patent

[31] A. Rabbani, M. Rokni, "Effect of nitrogen crossover on purging strategy in PEM fuel cell systems", Applied Energy, vol. 111, 1061-1070, 2013.

[32] K. Don Baik, M.S. Kim, "Characterization of nitrogen gas crossover through the membrane in proton-exchange membrane fuel cells", Int. J. Hydrogen Energy, vol. 36, 732-739, 2011.

[33] J. C. Amphlett, R. F. Mann, B. A. Peppley, P. R. Roberge, and A. Rodrigues, "A model predicting transient responses of proton exchange membrane fuel cells," Journal of Power Sources, vol. 61, no. 1–2. pp. 183–188, 1996, doi: 10.1016/S0378-7753(96)02360-9.

[34] F. Iester, L. Mantelli, M. Bozzolo, L. Magistri, A.F. Massardo, Performance Assessment of an Innovative Turbocharged Proton-Exchange Membrane Fuel Cell System ASME GT2023-103513

[35] L. Mantelli, F. Iester, S. Crosa, M. Bozzolo, L. Magistri, A.F. Massardo, Dynamic Performance Analysis of a turbocharged PEMFC System, ASME Turbo Expo 2024